European Journal of Forest Research (2023) 142:739–761
https://doi.org/10.1007/s10342-023-01553-0

ORIGINAL PAPER

Tower yarder powertrain performance simulation analysis: electrification study

Stefan Leitner[1] · Manuel Antonio Perez Estevez[1] · Massimiliano Renzi[1] · Raffaele Spinelli[2] · Fabrizio Mazzetto[1] · Renato Vidoni[1]

Received: 30 September 2022 / Revised: 8 February 2023 / Accepted: 1 March 2023 / Published online: 18 March 2023

Abstract

Radical changes are necessary to address challenges related to global warming and pollution. Ever-tightening emission standards for combustion engines have already led to a drastic reduction in the amount of harmful gas and matter emitted. Drivetrain hybridization and electrification, which are becoming increasingly popular in all sectors, are two additional ways to achieve that goal. However, within the forestry sector most of the equipments still rely on conventional mechanic or hydraulic drivetrains. An example of this is tower yarders, the workhorse of the alpine logging industry. This work simulates the duty cycle and energy flow of tower yarders in logging operations, both with conventional diesel–hydraulic configuration and a proposed hybrid configuration. The objective is to determine the potential of hybridized drivetrains for tower yarder applications. Detailed models are developed to describe the cable-based extraction of timber and tower yarder internal processes. Extensive simulations were performed to determine force, power and energy components during the harvesting operation for both the diesel–hydraulic and hybrid drivetrains. Results confirm the large potential of the hybrid configuration for efficiency improvement and emission reduction, with estimated fuel savings of 45% and 63% in the uphill and downhill configurations, respectively. Extensive sensitivity analysis further demonstrates that the hybrid concept remains effective across a wide range of cable setup and transport characteristics. This confirms the large potential of electrified drivetrains, especially in the presence of very dynamic duty cycles, as is the case in cable-based logging equipment.

Keywords Forest operations · Hybrid powertrains · Cable-based logging · Modeling · Energy efficiency

Communicated by Eric R. Labelle.

✉ Stefan Leitner
stefan.leitner@natec.unibz.it

Manuel Antonio Perez Estevez
mperezestevez@unibz.it

Massimiliano Renzi
massimiliano.renzi@unibz.it

Raffaele Spinelli
raffaele.spinelli@ibe.cnr.it

Fabrizio Mazzetto
fabrizio.mazzetto@unibz.it

Renato Vidoni
renato.vidoni@unibz.it

[1] Faculty of Science and Technology, Free University of Bozen-Bolzano, Piazza Università 5, 39100 Bozen, BZ, Italy

[2] Consiglio Nazionale delle Richerche-Istituto per la BioEconomia, CNR IBE, Via Madonna del Piano 10, 50019 Sesto Fiorentino, FI, Italy

Introduction

Global warming and air pollution have reached critical levels (Minderytė et al. 2022); therefore, their impact is becoming more evident every day. Vehicles are a major contributor in terms of greenhouse emissions and pollutants. Thus, regulations for vehicles have been introduced and became more stringent in the last years. Initially, these standards focused on on-road vehicles, but in recent decades they have extended to non-road vehicles, such as construction, agricultural and forestry machinery. EU Stage V in Europe (DieselNet 2021), EPA Tier 4 in the US EPA (2022) and emission standard IV for nonroad mobile machinery in China Shao (2021) are the standards that set the limits for different pollutants and thus the ones that force manufacturers to produce engines with advanced emission control technologies. Powertrain electrification is another solution that can reduce the carbon footprint of vehicles. The latter is widely used in passenger cars and buses; it may also be a

feasible solution for nonroad mobile machinery. In EU Stage V, engines with a power of less than 56 kW have lighter regulations, which makes engine downsizing through hybridization an interesting solution.

While several works have been done in this direction for agricultural applications, forestry applications lag developments in these broader markets. In fact, some early solutions of electric or hybrid tractors can already be found on the market and several conceptual designs are available in the literature (Troncon et al. 2019b; Medževepryte and Makaras 2018; Lagnelöv et al. 2021; Mendes et al. 2019; Troncon et al. 2019a; Dalboni et al. 2019), but just few studies about hybrid forestry machinery hybridization have been done. Mergl et al. (2021) studied the drivetrains of hybrid forestry equipment. Existing and emerging solutions were classified based on their hybridization concept in electro-hybrid, hydraulic hybrid or a combination of those. An additional classification in a parallel dimension was made in terms of series-hybrid, parallel hybrid, power split and fuel cell technology. The study further compared consumption and performance data of hybrid equipment on today's market. These include harvesters, woodchippers, wood trailers, forwarders and excavators with logging auxiliaries. All hybridization concepts proved to be beneficial for fuel consumption and emission reduction. Battery developments to date, application potential, suitability and challenges in various applications within the forestry sector were discussed in Pandur et al. (2021). In Karlušić et al. (2020), a quasi-static model of a forestry skidder is presented. Specifically, a parallel hybrid and conventional powertrain fuel consumption were compared. The authors indicate that fuel savings around 13.5% can be achieved with the proposed hybrid configuration and control strategy. Moreover, they estimate a payoff time of 46 months. Hybrid tree harvester concepts were studied in Rong-Feng et al. (2017) and Prochazka et al. (2019). Series hybrid electric concepts were proposed, and a design example based on a developed model and simulations was provided. All these studies suggest that benefits can be obtained through powertrain hybridization. Development with the help of models can represent an economical way to study different machinery configurations reducing the amount of prototypes needed, so their correct development and use can collaborate to the development of more sustainable forestry machinery. Theoretically, timber harvesting machinery has a considerable potential to be hybridized because of its well defined and repetitive working cycles, which most of the time require only little power compared to the peak power bursts. Moreover, during other periods exists the potential to recover a significant amount of energy. Currently, this is not possible because a mechanism capable to exploit braking power is needed, but conventional diesel–mechanic or diesel–hydraulic drivetrains are not well suited for that (Agwu Nnanna et al. 2015). In contrast, in electrified powertrains regenerative power can be recovered and stored. In addition, this type of powertrain can minimize idling losses.

A tower yarder (TY) is a type of forestry machinery for cable-based logging. The improvement in a tower yarder's powertrain could bring considerable environmental benefits in mountain areas where those machines are very popular. Despite this, to the knowledge of the authors, there exist few studies on their powertrain hybridization. Anyway, the interest for tower yarders among the scientific community has been increasing in the last decade and different studies about their economical aspects, productivity, safety and technical solutions and hazards can be found. Recently, a study about the design of hybrid tower yarder drivetrains has been published (Leitner et al. 2022b). The study gathered common duty cycle data of tower yarder operations from literature to define common and extreme working conditions as reference for the design of a hybrid tower yarder drivetrain. Design guidance, control algorithms and an example design of a 5-ton hybrid tower yarder are provided. However, the study does not investigate the efficiency of the proposed drivetrain, which is part of this work. Kühmaier et al. (2019) studied, by conducting an online survey, what tower yarder attributes would be desired by logging firms and equipment operators in New Zealand and Australia to achieve greater profitability in steep terrain logging. Talbot et al. (2015) assessed the benefits of a fully integrated yarder-processor against splitting the yarding and processing functions onto two base machines. Productivity and cost analysis indicate that there is no single optimal solution for all working conditions, but that it depends heavily on extraction distances and mean tree volumes among other factors. Schweier et al. (2020) also studied the productivity and costs of different commercially available tower yarder solutions. Similar studies are Spinelli et al. (2020), Munteanu et al. (2019) and Zimbalatti and Proto (2009), where how the degree of automation and the type of forest can affect performance and cost has been studied. Similar performance comparisons related to the choice of carriage in combination with tower yarders were performed for non-motorized versus motorized carriages in Spinelli et al. (2017a) and for conventional diesel–hydraulic versus electric energy-recuperating carriages in Varch et al. (2020). Gallo et al. (2021) presented an automated monitoring system for cable yarding systems, tested in various locations in Italy and New Zealand. The Geographical Navigation Satellite System (GNSS) coupled with a data-logging unit and a data analysis program enables to continuously monitor a cable yarder operation, providing the opportunity to manage and improve the system, as well as to study the effect on operations in different conditions. Monitoring and predicting skyline tensile forces and load paths are important for reasons of cost and safety and are discussed in Mologni et al. (2019) and Knobloch and Bont (2021), respectively. Spinelli et al. (2017b) offer a detailed insight into skyline

tensile forces during the hauling process and with various types of carriages (clamped and unclamped).

An energy efficiency study concerning a hybrid tower yarder (Koller K507e-H) from Koller Forsttechnik was recently published in Cadei et al. (2021). Four cable-based logging systems of various lengths were installed in uphill configuration to study fuel savings, energy need and energy recovery over a total of 915 transport cycles and about 212 h of operation. The average energy recovered was 2.56 kWh per transport cycle, amounting to a fuel saving of about 730 L in total during that period. Based on the data, models were derived expressing the net energy need and fuel consumption per transported payload as a function of yarding distance, clearly demonstrating the great potential of hybridization in this application. To the authors' understanding, the Koller K507e-H is a medium-sized tower yarder system and could be classified as a full-hybrid concept in series configuration (Govardhan 2017). It uses a 700 V based supercapacitor energy storage unit with a 35.8 kW diesel combustion engine driving a generator, controlled via a simple start-stop regime. The maximum forces of the winch systems are 25 kN (Cadei et al. 2021). This innovation represents an important first step toward the use of advanced drivetrains in tower yarders. However, some limitations still have to be overcome to make hybrid tower yarders applicable throughout the industry. The power and winch forces have to be increased by factors of about three and two, respectively. In addition, the current design may be a limiting factor of the maximum achievable efficiency during the transport process. Although not true for the duty cycles presented in the study, the energy storage system of the hybrid setup may not be able to buffer the full amount of energy available at particularly long or steep cable setups. In a previous work undertaken by the authors of this study (Leitner et al. 2022a), a model capable of estimating the power required by a large tower yarder in a typical working condition in alpine areas was introduced. This model was coupled to two different powertrain configurations: conventional and full hybrid, in order to estimate fuel consumption and study the potential benefits. The results show how the fuel efficiency could be improved by 45% and 63% for the uphill and downhill configuration, respectively. Still, information and understanding on how different parameters of tower yarder's duty cycles affect the energy consumption and thus the possibility of hybridization are missing in the literature.

The great potential for tower yarder's electrification and the lack of knowledge on this subject, together with tightening emission regulations, possible financial incentives for green machine fleets and growing environmental awareness of the entire value chain, point to the need to study in this direction. On this basis, the aims of this study are: (1) to give a detailed explanation of the feasibility of hybrid powertrains for tower yarders, (2) to suggest a control logic that can be used by the hybrid powertrain and (3) to understand how different environmental and working cycle variables of a large tower yarder (compatible with working practices of conventional 5-ton diesel–hydraulic tower yarders) can influence the power and energy required by the system, as well as the energy portion that can be recovered. This lasts in order to understand the hybridization potential in different operating conditions. In particular, this work studies in detail the impact of the pre-tensioning force, since it is one of the main sources of energy losses in this type of operation and, therefore, it is one of the critical parameters in terms of consumption.

Tower yarder's working principle

Tower yarders, as shown in Fig. 1, are the workhorse of the alpine logging industry today. They can handle virtually any slope and distances of up to about 800 m, in some cases significantly more. Tower yarders are semi-stationary winch systems. They differ from other winch systems used in alpine logging in that, for ease of transport, they are mounted on a trailer, independent tracked vehicle, tractor or truck. The most flexible versions include a skyline winch, two winches (mainline and haulback line) for the timber extraction process as well as a number of guyline and strawline winches. The tower provides one of the skyline's fixation points, which in turn is fixated to anchor points such as trees via the strawlines.

The three main drums of a tower yarder are the bulky skyline (SL) and a thinner mainline (ML) and haulback line (HL). To start the cable setup process, the skyline is wrapped off its drum and attached to one or multiple trees or artificial fixation points at the opposite end of the extraction corridor. The drum of the skyline is then capable of directly

Fig. 1 Tower yarder Mounty by Konrad Forsttechnik

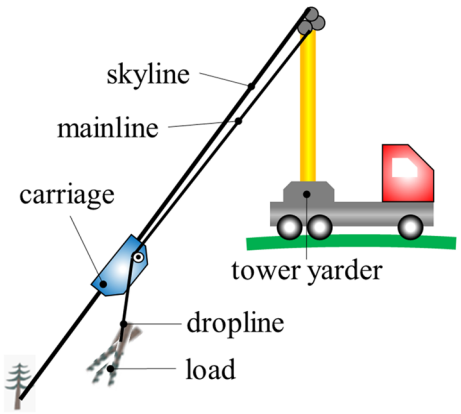

Fig. 2 Tower yarder in uphill configuration

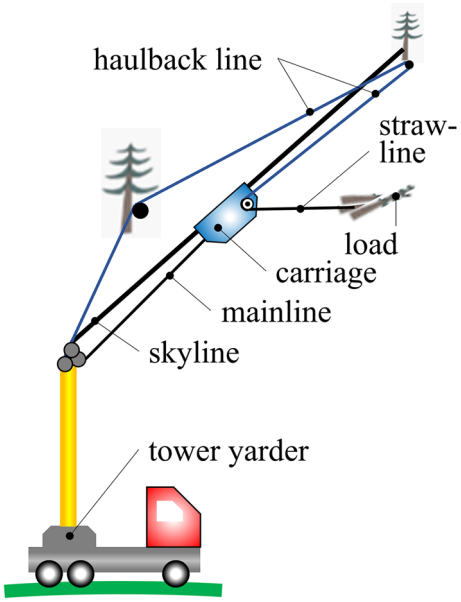

Fig. 3 Tower yarder in downhill configuration

tensioning the skyline. A so-called carriage is fed onto the skyline. The carriage is moving along the cable, carrying the logs from the felling site to an unloading point; its position is controlled by the mainline and haulback lines, as sketched in Figs. 2 and 3.

In conventional tower yarders, the drums are driven by independently controlled hydraulic motors with attached planetary reduction gears. The hydraulic motors are in turn driven by hydraulic pumps attached to a diesel engine. If the tower yarder is mounted on a tractor or truck, usually the base vehicle's engine is used to power the tower yarder. The engine tends to run nonstop for the entire workday. Its speed varies between idling speed when the tower yarder stands still and some fixed operating point when power is drawn by the tower yarder (Matthews 2021). Winch speed control is done via variable displacement hydraulic pumps and motors. Force limitation is achieved using pressure limitation valves, whereas the pressure thresholds are usually adjustable by the operators.

Tower yarder in uphill and downhill configuration

Uphill

As tower yarders are connected to some type of road vehicle, at least one of the endpoints of the cable must be accessible by the tower yarder base machine. If the cable is installed in an uphill configuration as in Fig. 2, the tower yarder is positioned at the cable's endpoint with higher elevation. This setup further requires sufficient slope for the carriage to move solely by gravity away from the tower yarder and toward the loading point. The carriage is connected to the tower yarder via the mainline, controlling its movement along the skyline. In addition, the mainline is often also used for lifting the load itself. Normally, the mainline passes through the carriage and ends in a hook or a T-shaped end connector for securing the slings that tie the load. The uphill yarding configuration represents the simplest and preferred cable setup.

Downhill

If the carriage with attached mainline does not move away from the tower yarder by gravity alone, the so-called downhill configuration depicted in Fig. 3 must be used. In the downhill configuration, the mainline and the haulback line form a closed loop. The mainline extends directly from the tower yarder to the carriage. The haulback line passes through a pulley at the opposite end of the cable before entering the carriage at the side facing away from the tower yarder. In this way, the tower yarder can pull the carriage in both directions via two independent winches. Since the carriage is located at a higher elevation than the tower yarder, the hook does not in general lower itself automatically as in the uphill configuration; several solutions exist to this problem and they go under the collective name of slack-pullers. Slack-pullers can be powered by the haulback line itself through a mechanical device or by a small independent motor, both internal to the carriage. Diesel-powered slack pullers have been the most common so far. However, in recent years, electric slack pullers have been introduced. The energy storage system is charged when spooling in the dropline. With dropline carriages, slack pulling challenges can be completely avoided. In that case, the carriage is fitted with its own independent winch, powered by a dedicated on-board engine through a hydrostatic transmission. Dropline spool-out and lateral yarding are handled solely by the carriage, while the tower yarder stands still during this

entire phase. To minimize carriage complexity and weight, the tower yarder can still be used to accomplish this task. Such solutions usually work with multiple drums in the carriage, all mechanically connected to each other, as sketched in Fig. 4. Usually, the carriage contains three drums for the mainline, haulback line and dropline, respectively. By locking the carriage in place via a skyline brake and by opening the drum brake in the carriage, dropline is spooled out by spooling mainline cable off its drum in the carriage. The dropline lowers to the ground. When lifting the payload via the haulback line, the mainline is spooled back onto its drum. For the sake of this study, a simple non-automated carriage with three integrated drums is considered. Examples are the LW TST 3500/I or LW TST 5000/I models from TST forestry. Since the carriage does not contain any source of energy, all work done during cable extraction is powered by the tower yarder. Due to this simplification, analysis of energy flow and fuel consumption is limited to the yarder only. For the subsequent discussion, it is sufficient to understand that mainline and haulback line are responsible to lower and lift the hook, respectively. Since there exist only comparably few dropline carriages, and since slack pulling draws only a small percentage of overall cycle energy, these results hold for the majority of equipment combinations employed today.

Naturally, the installation of a downhill configuration is more cumbersome than the installation of an uphill configuration. It is very simple to position the tower yarder at the upper end of the cableway and pull the lines down by hand. In the downhill configuration, installation or strawline winches are needed. One cable after the other must be pulled uphill. It can also be expected that energy losses are significantly larger in the downhill setup, due to long moving cables and the need for pre-tension in the loop of cables to maintain the lines in good condition for long term. This is also necessary to guarantee smooth carriage travel, without any "jerking" motion. This tension is achieved through the loop formed by the mainline and haulback lines. Whichever drum is spooling cable off introduces a retarding force. For example, when moving the carriage uphill, the carriage is pulled by the haulback line. The wrapped-off mainline applies a certain pretension to keep both lines under tension. Similarly, when moving the carriage downhill by the mainline, the haulback line applies a certain pretension. This pretension is achieved via a so-called mooring valve, which controls braking torque build-up based on a differential pressure measurement. The pretension pressure setpoint is usually controlled by the operator based on experience. Apart from these deliberately introduced losses, long moving cables in the downhill configuration lead also to significantly higher friction losses during operation. It is part of this work to quantify these losses. Therefore, and because of the greater installation effort, the uphill configuration is usually the setup of choice, if the geographical conditions permit it. From an energetic point of view, this does not make sense. During the harvesting process, the tower yarder transports the timber uphill, sometimes spanning several hundreds of meters of elevation difference. In a second step, the timber is then transported down by some road vehicle.

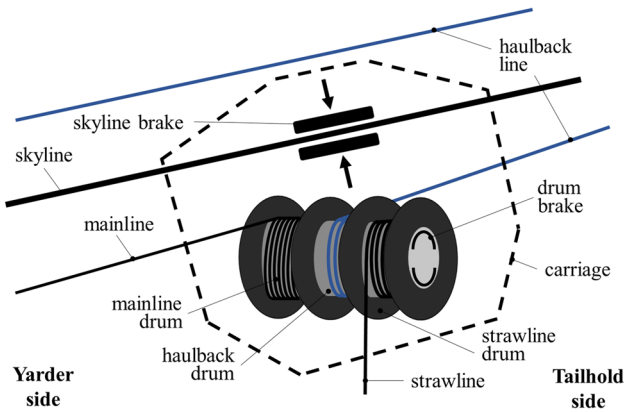

Fig. 4 Basic working principle of associated multi-drum carriage—Haulback and mainline drum within the carriage

System modeling

This section describes the equations used to model the operation of a tower yarder, specifically, in its two possible configurations: uphill and downhill. For these cases, a quasi-static single point model has been developed, the acceleration and deceleration have been neglected, and it was assumed that the forces of a body are concentrated at a single point. Such approximations are expected to have a minor impact on the overall results in terms of energy, as the duration of this phenomena is small compared to the rest of the cycle (Leitner et al. 2022b). On the same basis, the model also neglects the internal and external disturbances that generate variations on the actual load profile.

A single payload transport cycle in both configurations was divided into eight work phases (WPs), where the ith work phase ends at time t_i. The actions taken in each work phase are described in Table 1. The length of each work phase is defined by the amount of cable to be spooled off or onto the winch drums (distance covered by the carriage) and the drum's speed, which is an operator input or limited by the tower yarder's maximum power. Standstill periods depend on many factors (such as the number and experience of available workers, terrain and weather conditions, type and size of logs, etc.) and are inputs to the model. Forces, power and energy levels are computed separately for each work phase and independently for the uphill and downhill configuration.

Table 1 Work phases (WPs) of a single logging transport cycle (uphill and downhill)

Denotation	Time	Description
Outhauling	$0 - t_1$ (WP1)	Moving the carriage from the yarder to the loading site (movement downhill/uphill in the uphill/downhill configuration, respectively)
Lower hook	$t_1 - t_2$ (WP2)	Lowering of the lifting hook to reach the payload to be transported
Attach payload	$t_2 - t_3$ (WP3)	Attaching of the payload to the lifting hook
Lift payload	$t_3 - t_{4_C}$ (WP4)	Lifting the payload (at felling site) consists of:
		• $t_3 - t_{4_A}$: pulling the spread-out payload below the carriage
		• $t_{4_A} - t_{4_B}$: lifting the payload (at least partially) off the ground
		• $t_{4_B} - t_{4_C}$: lifting the payload all the way up to the carriage (may be 0 if the load is only partially lifted)
Inhauling	$t_{4_C} - t_5$ (WP5)	Movement of the loaded carriage from the felling site to the yarder (movement uphill/downhill in the uphill/downhill configuration, respectively)
Lower payload	$t_5 - t_{6_B}$ (WP6)	Lowering of the payload to the ground (at landing point) consists of:
		• t_{6_A}: lowering the payload until it touches the ground (may be 0 if the load is just partially lifted)
		• t_{6_B}: lowering the payload all the way to the ground
Detach payload	$t_{6_B} - t_7$ (WP7)	Detach the payload from the lifting hook
Lift hook	$t_7 - t_8$ (WP8)	Lifting the hook off the ground

Although in practice the forces suffer variations due to various disturbances, i.e., obstacles along the corridor, it has been assumed that the forces remain constant for each work phase. Some system behaviors were considered by conditional statements rather than simple closed form expressions. Examples are whether the payload is fully suspended in work phases 4 and 6 and the value of the counteracting force controlled by the mooring valve in work phases 5 and 6 in downhill configuration, which depends on many factors.

Yarding uphill

This subsection describes the model developed for the transport uphill. This setup makes use of the mainline, the haul-back line remaining unused. Therefore, all forces, power and energy levels in this section correspond to the drive of the mainline drum. Figure 5a, b shows the forces of mainline and dropline (payload) acting on the carriage suspended on an inclined skyline during work phases 1 (outhauling) and 5 (inhauling), respectively. The corresponding equations for

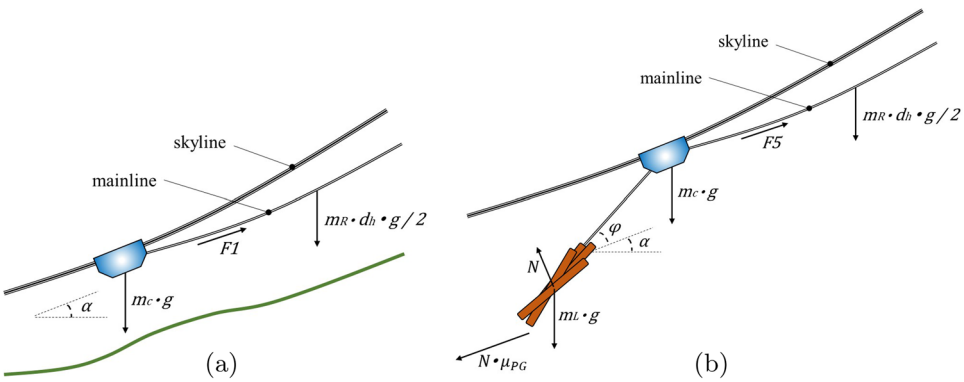

Fig. 5 Scheme of the forces acting on the suspended carriage during uphill transport in work phase 1 (**a**) and 5 (**b**). The variables are defined as follows: α—slope of the terrain; m_C—carriage mass; g—gravity; m_R—mass of the mainline cable per unit length; d_h—mainline cable length between tower yarder and carriage at loading point; φ—angle between terrain and dropline (smaller 90°); m_L—payload mass; μ_{PG}—friction coefficient between payload and ground; N—normal force payload to ground; $F_1 \ldots F_8$—mainline cable forces in work phases WP1 ...WP8

Table 2 Equations to model uphill transport

Work phase	Denotation	Mathematical description
$0 - t_1$	Outhauling	$F_1 = (m_C + \frac{m_R d_h}{2}) g \sin(\alpha)$
$t_1 - t_2$	Lower hook	$F_2 = m_R d_h g \sin(\alpha)$
$t_2 - t_3$	Attach payload	$F_3 = 0$
$t_3 - t_4$	Lift payload	$F_{4_A} = m_L g \mu_{PG} + m_R d_h g \sin(\alpha)$
		$F_{4_{Bi}} = \frac{m_L g sin(\alpha) + cos(\alpha)\mu_{PG}}{\sin(\varphi)+\cos(\varphi)\mu_{PG}} + m_R d_h g \sin(\alpha)$
		$F_{4_C} = m_L g + m_R d_h g \sin(\alpha)$
$t_4 - t_5$	Inhauling	$F_5 = m_C + m_L + \frac{m_R d_h}{2} g \sin(\alpha)$ (FS)
		$F_5 = \frac{m_C + \frac{m_R d_h}{2} g \sin(\alpha) + m_L g \cos(\varphi)(\sin(\alpha)+\cos(\alpha)\mu_{PG})}{\cos(\varphi)+\sin(\varphi)\mu_{PG}}$ (SS)
$t_5 - t_6$	Lower payload	$F_{6_A} = m_L g \quad F_{6_B i} = \frac{m_L g \sin(\alpha)}{\cos(\varphi)}$
$t_6 - t_7$	Detach payload	$F_7 = 0$
$t_7 - t_8$	Lift hook	$F_8 = 0$

each work phase are given in Table 2, where F_i is the force at the mainline and the subindex i corresponds to the specific work phase, m_C and m_L are the mass of the carriage and load, respectively, m_R is the mass of the mainline per unit length, d_h is the maximum distance between the carriage and the tower yarder within the given work phase, g is the gravity, N is the normal force and μ_{PG} is the friction coefficient between the ground and the load. α and φ are, respectively, the terrain's slope and the angle between the terrain and the section of cable connecting the load to the carriage. α is an input to the model. φ is computed based on expressions:

$$\varphi = 90 - \alpha \tag{1}$$

$$\varphi = a \sin\left(\frac{h}{L}\right) \tag{2}$$

for the cases fully suspended (FS) and semi-suspended (SS), respectively. In the FS case, the dropline has vertical orientation, in which case φ is maximized. In the SS case, the dropline deviates from vertical orientation, such that φ becomes smaller with respect to the FS case (as depicted in Fig. 5b). h is the height of the skyline above the ground, and L is the length of the lifting hook and logs combined. All parameters are assumed constant during each work phase.

In work phase 1, the carriage moves down the skyline by the force of gravity. The amount of mainline along the corridor is equal to the carriage's distance from the tower yarder. For the sake of this quasi-static model, the mainline length considered in the derivations is the average distance between the carriage and the tower yarder in the given work phase, which corresponds to half of the maximum distance in work phase 1. Minor losses such as cable friction on the ground or rolling resistance and losses in pulleys are not considered. In work phase 2, only the mass of the mainline contributes a force. The cable section between tower yarder and carriage is considered, while the section between carriage and hook is ignored. Lifting or lateral yarding (work phase 4) is made up of three sub-windows, as reported in Table 1. During the first phase, denoted by subindex A, the payload is dragged from the felling site to below the carriage. The payload can be spread out 100 m or more to the left or right of the carriage. The mass of the moving mainline and the friction of the payload on the ground are considered. That is very important, because friction at the breakout phase can be very high (often due to the log ends being hung-up against some obstacles, and or the branches in case of full tree extraction can be entangled with the branches of other adjacent trees). In the second phase (subindex B), the payload is lifted off the ground. F_{4B} was estimated as the average between the forces when the payload starts to become airborne ($\varphi = 0$) and the force at the end of the lifting phase. Lifting phase B ends when the load no longer touches the ground, or, in case the load is semi-suspended, when the lifting process ends. Each of the forces $F_{4_{Bi}}$ can be estimated as given in Table 2. In practice, the length of the hook and the length of the logs combined are often longer than the clearance of the skyline. In case the payload is fully suspended, F_{4_C} equates to the force required to lift the payload up vertically. The winch force during inhauling (work phase 5) is also highly dependent on whether the load is FS or SS. In the former case, the force is made up by the movement of the carriage, the payload and the mainline uphill. In the latter case, ground friction becomes an additional factor.

Similar to work phase 4, work phase 6 may or may not consist of a phase where the load is fully suspended. F_{6_A} may thus be 0 or corresponds to the vertical lowering of the payload. F_{6_B} is defined to be the average of the forces between when the payload starts to touch the ground and just before being fully lowered. In this case, the friction force has been ignored. The power consumed for lifting the hook in work phase 8 has been neglected. The amount of mainline in motion in work phases 6–8 is small and thus ignored as well.

Instantaneous mechanical power at the winch drums follows from the product of cable speed and cable tension, as given by Eq. 3. As the tension of the cables always points

in the same direction, the sign of the winch speed v_i directly determines the sign of the power, whereas positive and negative power correspond to motoring and generating power, respectively. Mechanical energy at the drum results from drum power and the work phase duration (Eq. 4). Duration is a function of operating speeds, distances to be covered and idling periods, all inputs to the model.

$$P_{\text{mech}_i} = F_i v_i \tag{3}$$

$$E_i = P_{\text{mech}_i} t_i \tag{4}$$

Logging downhill

This subsection describes the model developed for the transport downhill. This setup makes use of both the mainline and the haulback line. In the downhill configuration, the mainline and the haulback line form a closed loop between the tower yarder, carriage and a pulley at the other end of the corridor. Regardless of the position of the carriage along the skyline, the length of cable in motion at any given moment is constant. In practice, mainline and haulback line may differ in diameter by a millimetre or two. By ignoring this detail, the mass of the cables has not been longer considered in the subsequent derivations.

Cable friction, on the other hand, is much more significant in the downhill configuration. The cable in motion is in the order of twice the length of the skyline. Pulleys installed at critical points help to mitigate friction. It is, however, not uncommon that the tensioned cable is deflected at contact points with the ground, trees or other obstacles. This deflection is modeled via the fundamental belt friction equation (Eq. 5), also exploited in the study of the capstan equation (Starkey and Williams 2011) and explained with the help of Fig. 6. μ_{LG} is the friction coefficient between the terrain and the cable, and β the deflection angle of the cable.

$$F_b = F_a e^{\mu_{\text{LG}}\beta} \tag{5}$$

Forces, power and energy levels are computed for the mainline and haulback drums in every work phase. Again, for exemplary purposes, key forces and force allocations in work phases 1 and 5 are depicted in Fig. 7. The corresponding equations for downhill logging process are given in Table 3, where F_{M} is the resulting counter force applied by the mooring valve.

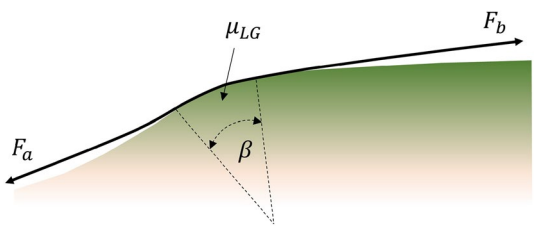

Fig. 6 Modeling friction due to cable deflection by a fixed obstacle

In work phase 1, the mainline slows down the upward movement of the carriage via the mooring valve. $F_{\text{M}_{\text{ML}}}$ is selected by the operator. The haulback line has to overcome the force in the mainline, the mass of the carriage and the frictional losses in the haulback line and mainline. When lowering the hook in work phase 2, the haulback line ensures cable tension via the mooring valve. The mainline must work against this force, heightened by the frictional losses. Forces in work phase 4 (lateral yarding) are modeled similarly to those in work phase 4 of the uphill configuration, but in this case must be considered the force added by the mainline to ensure cable tension and the cable's frictional term. The length of cable in motion along the skyline is constant, and therefore, the force due to its weight is ignored.

In work phases 1, 2 and 4, the cable pre-tensioning setpoint is associated with the mainline, haulback line and again the mainline, respectively. The pre-tensioning condition is guaranteed because all the forces in the system point in the same direction, as can be seen in the equations of Table 3. Therefore, it is clear that the force calculated in the drum in motor mode is higher than the minimum pre-tensioning force required for the cables to wind smoothly, and moreover, it is positive and thus has physical coherence because cables can just pull. The motor mode force corresponds to the haulback line, mainline and haulback line drum in work phases 1, 2 and 4, respectively. In work phases 5 and 6, this is not the case. In work phase 5, the gravitational force of the loaded carriage on the sloped skyline and the force of the haulback line with associated friction point are in opposite directions. As a result, a fixed relationship between the pre-tensioning force and the haulback line can only be established, if the mainline force is no smaller than the pre-tensioning force, given the pre-tensioning force in the haulback line. Otherwise, force control has to be performed at the haulback line to achieve the pre-tensioning force at the mainline. In work phase 6, the gravitational force of the payload works against the force in the haulback line and its friction. Again, the minimum required tension in the mainline may not be reached, in which case the force in the haulback line is raised accordingly. In the same way as for the uphill configuration, the power and energy were computed using Eqs. 3 and 4.

Tower yarder traditional drivetrain

The tower yarder is powered by a diesel internal combustion engine (ICE) driving hydraulic pumps (PUM), which in turn drive the winch drums (mainline drive MLD and haulback drive HBD) via hydraulic motors (MOT) and an intermediary planetary reduction gear, as shown in the

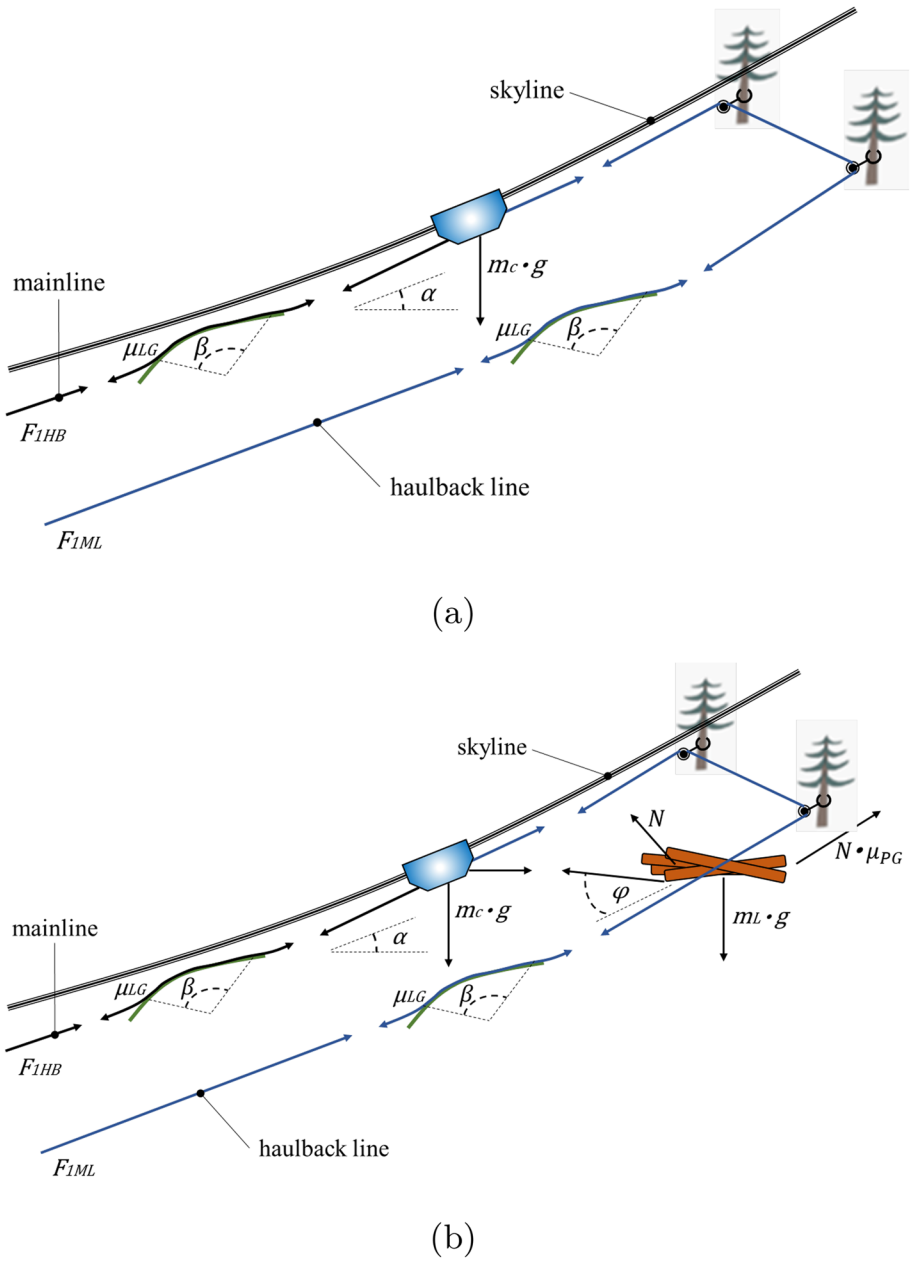

Fig. 7 Scheme of the key forces acting on the suspended carriage during downhill transport in work phase 1 (**a**) and 5 (**b**)

scheme of Fig. 8. All drivetrain losses of the hydraulic system are summarized as an average drivetrain efficiency denoted by η_{HY}. Then, the power at the engines' crankshaft can be calculated as:

$$P_{ICE} = \begin{cases} \frac{P_{mechanical}}{\eta_{HY}} & \text{if } \frac{P_{mechanical}}{\eta_{HY}} > P_{idling} \\ P_{idling} & \text{if } \frac{P_{mechanical}}{\eta_{HY}} < P_{idling} \end{cases} \quad (6)$$

If the mechanical power at a drum is negative, it is dissipated hydraulically with the help of mooring valves (MOORING). Thus, the drives are not driving the engine, which runs at some idling power P_{idling} at idling speed. The engine has been modeled according to the polynomial equations in Ben-Chaim et al. (2013), which are again reported in Eqs. 7–11 below. Specifically, this model was built by decoupling the speed and power influence on the efficiency by employing two single dimension polynomials. The model has been fitted and verified using a data set of different vehicles (type and size). This generic model allows to simulate engines of different sizes, by just giving few input data. The engine efficiency η_{ICE} and fuel consumption (Q) can be calculated using the following equations:

Table 3 Equations to model downhill transport

Work phase	Denotation	Mathematical description
$0-t_1$	Outhauling (uphill)	$F_{1_{\mathrm{ML}}}=F_{\mathrm{M_{ML}}}\quad F_{1_{\mathrm{HB}}}=(m_{\mathrm{C}}g\sin(\alpha)+F_{1_{\mathrm{ML}}}\mathrm{e}^{\mu_{\mathrm{LG}}\beta})\mathrm{e}^{\mu_{\mathrm{LG}}\beta}$
t_1-t_2	Lower hook	$F_{2_{\mathrm{HB}}}=F_{\mathrm{M_{HB}}}\quad F_{2_{\mathrm{ML}}}=F_{2_{\mathrm{HB}}}\mathrm{e}^{2\mu_{\mathrm{LG}}\beta}$
t_2-t_3	Attach payload	$F_{3_{\mathrm{ML}}}=0\quad F_{3_{\mathrm{HB}}}=0$
t_3-t_4	Lift payload	$F_{4_{\mathrm{ML}}}=F_{\mathrm{M_{ML}}}$
		$F_{4_{HB_A}}=m_{\mathrm{L}}g\mu_{PG}+F_{4_{\mathrm{ML}}}\mathrm{e}^{\mu_{\mathrm{LG}}\beta}\mathrm{e}^{\mu_{\mathrm{LG}}\beta}$
		$F_{4_{HB_{Bi}}}=(\frac{m_{\mathrm{L}}g(\sin(\alpha)+\cos(\alpha)\mu_{PG})}{\cos(\varphi)+\sin(\varphi)\mu_{PG}}+F_{4_{\mathrm{ML}}}\mathrm{e}^{\mu_{\mathrm{LG}}\beta})\mathrm{e}^{\mu_{\mathrm{LG}}\beta}$
		$F_{4_{HB_C}}=(m_{\mathrm{L}}g+F_{4_{\mathrm{ML}}}\mathrm{e}^{\mu_{\mathrm{LG}}\beta})\mathrm{e}^{\mu_{\mathrm{LG}}\beta}$
t_4-t_5	Inhauling (downhill)	$F_{5_{\mathrm{HB}}}=F_{\mathrm{M_{HB}}}$
		$F_{5_{\mathrm{ML}}}=(-(m_{\mathrm{C}}+m_{\mathrm{L}})g\sin(\alpha)+F_{5_{\mathrm{HB}}}\mathrm{e}^{\mu_{\mathrm{LG}}\beta})\mathrm{e}^{\mu_{\mathrm{LG}}\beta}\ (FS)$
		$F_{5_{\mathrm{ML}}}=(-m_{\mathrm{C}}g\sin(\alpha)+\frac{m_{\mathrm{L}}g(\cos(\varphi)\cos(\alpha)\mu_{PG}-\sin(\varphi))}{\cos(\varphi)+\sin(\varphi)\mu_{PG}}+F_{5_{\mathrm{HB}}}\mathrm{e}^{\mu_{\mathrm{LG}}\beta})\mathrm{e}^{\mu_{\mathrm{LG}}\beta}\ (SS)$
		$Case\ F_{5_{\mathrm{ML}}}<F_{\mathrm{M_{ML}}}$
		$F_{5_{\mathrm{ML}}}=F_{\mathrm{M_{ML}}}$
		$F_{5_{\mathrm{HB}}}=\frac{(m_{\mathrm{C}}+m_{\mathrm{L}})g\sin(\alpha)\mathrm{e}^{\mu_{\mathrm{LG}}\beta}+F_{5_{\mathrm{ML}}}}{\mathrm{e}^{2\mu_{\mathrm{LG}}\beta}}\ (FS)$
		$F_{5_{\mathrm{HB}}}=\frac{F_{5_{\mathrm{ML}}}}{\mathrm{e}^{2\mu_{\mathrm{LG}}\beta}}+\frac{m_{\mathrm{C}}g\sin(\alpha)-\frac{m_{\mathrm{L}}g\cos(\varphi)(\cos(\alpha)\mu_{PG}-\sin(\alpha))}{\cos(\varphi)+\sin(\varphi)\mu_{PG}}}{\mathrm{e}^{\mu_{\mathrm{LG}}\beta}}\ (SS)$
t_5-t_6	Lower payload	$F_{6_{HB_A}}=F_{\mathrm{M_{HB}}}$
		$F_{6_{ML_A}}=-m_{\mathrm{L}}g+F_{6_{HB_A}}\mathrm{e}^{\mu_{\mathrm{LG}}\beta}\mathrm{e}^{\mu_{\mathrm{LG}}\beta}$
		$CaseF6ML<FMML$
		$F_{6_{ML_A}}=F_{\mathrm{M_{ML}}}$
		$F_{6_{HB_A}}=\frac{F_{6_{ML_A}}}{\mathrm{e}^{2\mu_{\mathrm{LG}}\beta}}+\frac{m_{\mathrm{L}}g}{\mathrm{e}^{\mu_{\mathrm{LG}}\beta}}$
		$F_{6_{HB_B}}=F_{\mathrm{M_{HB}}}$
		$F_{6_{ML_{Bi}}}=\frac{-m_{\mathrm{L}}g\sin(\alpha)}{\cos(\varphi)}+F_{6_{HB_B}}\mathrm{e}^{2\mu_{\mathrm{LG}}\beta}$
		$F_{6_{ML_B}}=F_{\mathrm{M_{ML}}}$
		$F_{6_{HB_B}}=\frac{2F_{6_{ML_B}}+(\frac{1}{\cos(\varphi)}+1)(m_{\mathrm{L}}g\sin(\alpha)}{2\mathrm{e}^{2\mu_{\mathrm{LG}}\beta}}$
t_6-t_7	Detach payload	$F_{7_{\mathrm{ML}}}=0\quad F_{7_{\mathrm{HB}}}=0$
t_7-t_8	Lift hook	$F_{8_{\mathrm{ML}}}=F_{\mathrm{M_{ML}}}\quad F_{8_{\mathrm{HB}}}=F_{8_{\mathrm{ML}}}\mathrm{e}^{2\mu_{\mathrm{LG}}\beta}$

$$\eta_{\mathrm{ICE}}=\eta_{\mathrm{o}}\mu_{\mathrm{p}}\mu_{\mathrm{n}} \tag{7}$$

$$\mu_{\mathrm{p}}=0.597-0.167\frac{P_{\mathrm{ICE}}}{P_{\mathrm{e}}}+2.496\left(\frac{P_{\mathrm{ICE}}}{P_{\mathrm{e}}}\right)^2-2.113\left(\frac{P_{\mathrm{ICE}}}{P_{\mathrm{e}}}\right)^3 \tag{8}$$

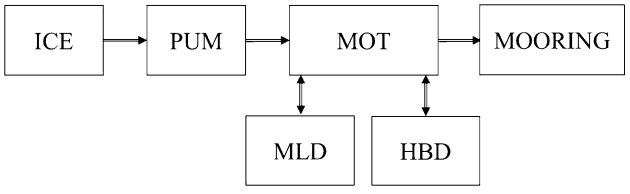

Fig. 8 Building blocks of the traditional tower yarder drivetrain . The abbreviations are defined as follows: *ICE* internal combustion engine, *PUM* (hydraulic) pumps, *MOT* (hydraulic) motors, *MOORING* mooring valves, *MLD* mainline drive, *HBD* haulback drive

$$\mu_{\mathrm{n}}=0.7107+0.9963\frac{n_{\mathrm{i}}}{n_{\mathrm{e}}}-1.0582\left(\frac{n_{\mathrm{i}}}{n_{\mathrm{e}}}\right)^2+0.3124\left(\frac{n_{\mathrm{i}}}{n_{\mathrm{e}}}\right)^3 \tag{9}$$

$$Q=\frac{P_{\mathrm{ICE}}}{\eta_{\mathrm{ICE}}C_{\mathrm{p}}} \tag{10}$$

where η_{o} is the engine nominal efficiency, n_{i} is the instantaneous speed, n_{p} is the speed corresponding to the engine rated power, C_{p} is the calorific power of diesel and P_{e} is the maximum engine power at the corresponding instantaneous velocity. In this work, the maximum power curve of the engine has been approximated using Eq. 11 (P_{p} is the engine rated power), which was obtained by fitting the engine of DEUTZ (2021). The total volume of fuel consumed in one

cycle can be calculated as the integral of the fuel consumption rate.

$$P_e = P_p\left(-0.041\left(\frac{n_i}{n_p}\right)^3 - 0.563\left(\frac{n_i}{n_p}\right)^2 + 1.765\frac{n_i}{n_p} - 0.165\right) \quad (11)$$

Hybrid drivetrain

The conventional tower yarder drivetrain was compared with the series hybrid version proposed in this work to unveil the true potential for energy recovery and efficiency improvement. In the hybridized concept, hydraulic motors are replaced by electric motors. A high-power energy storage system (ESS) supplies and absorbs energy to and from the mainline drive and haulback drive via dedicated inverters during the highly dynamic load profile. An internal combustion engine supplies energy to the system by acting on an additional generator– inverter (GR) set, collectively denoted as genset (GS). All power electronic components and the energy storage system are interconnected at the power distribution unit (PDU). Figure 9a shows the main building blocks of the hybrid tower yarder system and their interconnections. In Fig. 9 is also shown the direction of the power in all eight work phases, when operating in uphill configuration. Arrows indicate the presence and direction of energy flow, whereas the arrow's colors represent:

- *Black* genset energy, genset most likely active
- *Gray* genset energy, genset possibly active
- *Orange* drum motoring/battery discharge power
- *Green* drum generating/battery charge power

The mainline drive is generally driven by the downward movement of the carriage and the load being lowered in work phases 1 and 6, respectively (Fig. 9c). The mainline drive draws power in work phases 4 and 5 to lift the payload and transport it uphill (Fig. 9b). In work phases 2, 3, 7 and 8, power is minimal or zero (Fig. 9d).

The power of the genset adds to the charging power delivered by the mainline drive or subtracts from the discharge power the energy storage system delivers to the mainline drive. Naturally, it is of advantage to have the genset active when the mainline drive draws power and to shut it off when the mainline drive is in generator mode. A very simple genset control strategy to implement for uphill transport is to activate the genset at the beginning of work phase 4, and it can run at its maximum efficiency point until the previous cycle's net energy consumption has been compensated, which probably is similar to the current one. If the continuous operation at the maximum efficiency point is not enough to provide net energy need, a decision has to be made between most efficient operation (compromised performance) and maximum performance operation (compromised efficiency), running the genset at its maximum performance point. The described strategy is the one used in

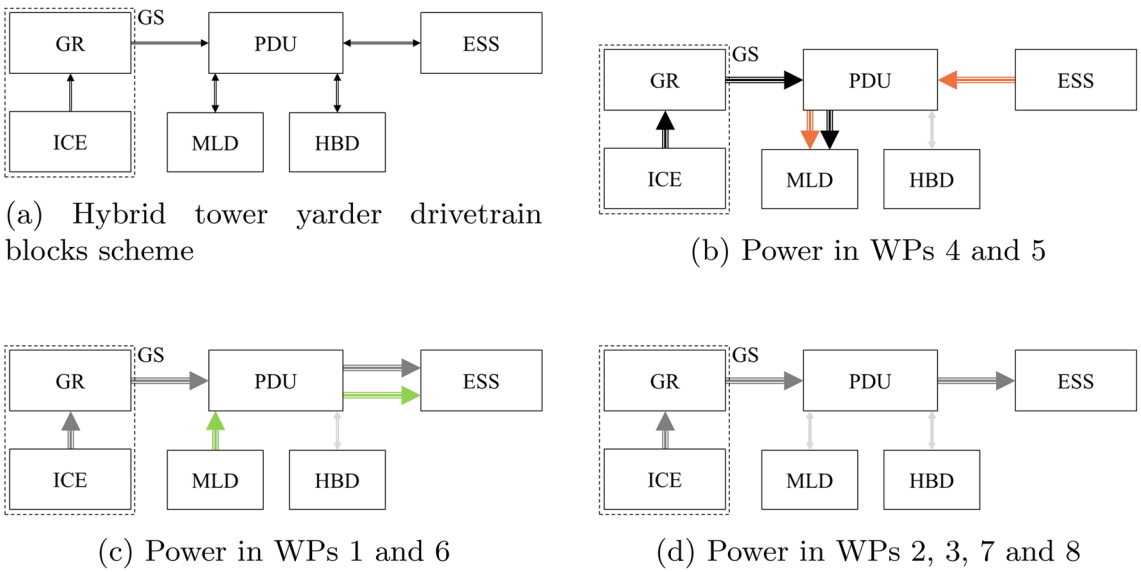

(a) Hybrid tower yarder drivetrain blocks scheme

(b) Power in WPs 4 and 5

(c) Power in WPs 1 and 6

(d) Power in WPs 2, 3, 7 and 8

Fig. 9 Building blocks, interconnections and power direction in work phases 1–8 in the proposed hybrid tower yarder drivetrain in uphill transport. The abbreviations are defined as follows: *ICE* internal combustion engine, *GR* electric generator and inverter (power electronics), *GS* genset (the combination of combustion engine, generator and inverter forming an electric energy source), *PDU* power distribution unit, *ESS* energy storage system, *MLD* mainline drive, *HBD* haulback drive

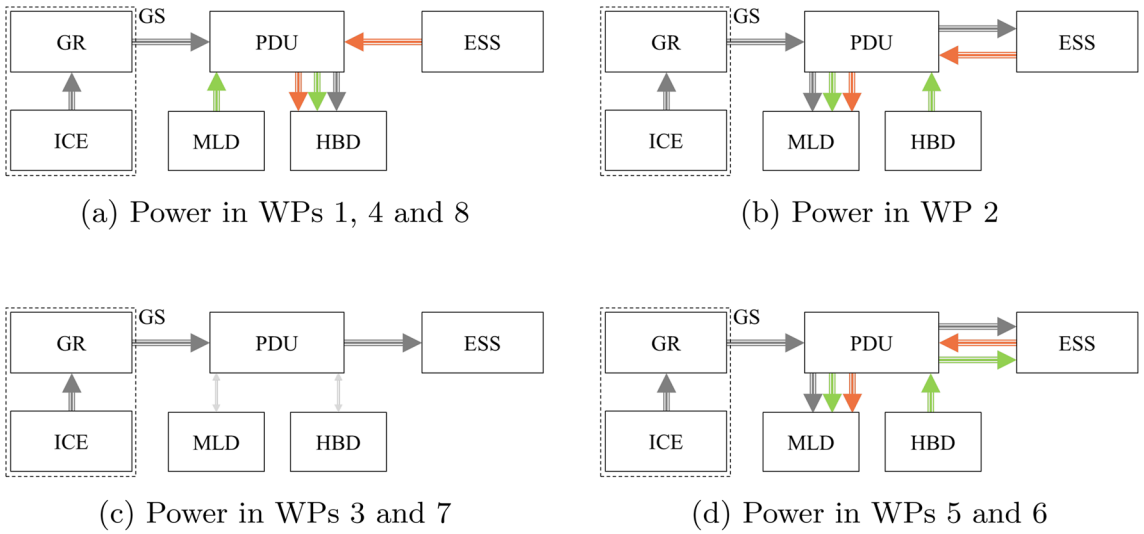

Fig. 10 Building blocks, interconnections and power direction in work phases 1–8 in the proposed hybrid tower yarder drivetrain in downhill transport. See Fig. 9 for definitions of the abbreviations

this work. More advanced control algorithms could further improve overall efficiency.

Figure 10 shows the power direction in all eight work phases when operating in downhill configuration. This makes use of both the mainline drive and the haulback drive. When working with a standard clamped carriage, the mainline drive and haulback drive are always moving together but in opposing directions observed from the tower yarder. Naturally, one of the drives is operating in motor mode and the other in generator mode at any time, when active. Figure 10a shows the flow of energy in the three work phases, where the haulback drive is in motoring mode. This is the case when hauling out in work phase 1, when lifting the payload in work phase 4 and when lifting the empty hook in work phase 8. In these work phases, the mainline drive ensures cable tension and operates in generator mode. Assuming the genset being off, the energy storage system is discharged during these phases. Work phase 2, shown in Fig. 10b, is an instance where the energy storage system is surely discharged, if the genset is inactive. Haulback drive and mainline drive directions invert to lower the hook. The tower yarder stands still in work phases 3 and 7 (Fig. 10c). In work phases 5 and 6 (Fig. 10d), the direction of energy flow in the energy storage system is unknown. Mainline drive motoring power may dominate over regenerative power of the haulback drive when the terrain's slope is small, the payload is dragged rather than fully suspended, or there is lots of friction along mainline and haulback line. In this case, downward transport will require significant energy delivered by the genset. If the downward movement of the carriage is propelled by the gravitational force of carriage and payload, regenerative power at the haulback drive can exceed mainline drive motoring power, leading to the energy storage system being recharged. This leads to fuel savings and possibly even energy autarkic operation, if enough energy can be recovered in these work phases.

Considerations made for the control of the genset in uphill configuration hold also in this case. The ideal point to start the genset appears to be at the beginning of work phase 1, as work phases 1 and 2 are guaranteed to be net motoring phases, followed by a standstill phase in work phase 3 and another motoring phase in work phase 4.

So far, it has not been discussed how the hybrid tower yarder would cope with operation beyond energy autarky. If net energy consumption is "negative" for a complete cycle, the state of charge (SOC) of the storage system will increase. Reached a certain maximum SOC, the tower yarder will have to be stopped and energy will be extracted via some type of energy dissipation unit. However, due to the losses associated with the transport process itself, it is unlikely that this might be a regular occurrence and is therefore not further considered.

As will become apparent from simulation results, the energy need per cycle both in uphill and downhill transports is at most a few kWh. Logging jobs observed in Cadei et al. (2021), for example, consumed at most 1.15 kWh of energy during the transport uphill and no more than 0.5 kWh in the remaining phases combined to finish a complete transport cycle. Based on the design of most modern tower yarders, it is reasonable to assume that a demanding logging job with medium- to large-sized machine may require a maximum power of more than 100 kW at the winch systems. Battery systems, supercapacitors, flywheels or a combination of

these may make up the energy storage system, without this changing the general results of this work. In case an energy dense storage solution is employed (most battery systems), power becomes the design factor. This requires the battery to be oversized with respect to the energy need to meet the power requirements. Supercapacitors, whose energy density is orders of magnitude below that of advanced batteries, would most likely have to be designed based on total cycle energy need. At the current storage technology status, a well-designed flywheel system may result in the best trade-off between power and energy density for this particular application, as well as guarantee high cycle life.

The system concept proposed above operates in a way to maximize efficiency and minimize genset starts, while keeping control complexity at a minimum. This differs from the Koller K507e-H in which the energy storage system would be designed with a large capacity that could deliver enough energy for one or more complete cycles. This opens up significant flexibility for genset control and overall system performance optimization. Whenever possible, energy is recovered and stored in the energy storage system. In the downhill configuration, this may result in autarkic operation. In the uphill configuration, and in most downhill configurations, additional energy is supplied into the system by the genset. To minimize energy storage system power and energy throughput, the genset is ideally activated when large power is drawn from the energy storage system, as described above. The genset is then active until enough energy is obtained to complete the transport cycle—compensating for the difference of cycle energy need and regenerative energy. The genset engine constantly operates at its maximum efficiency point to boost overall efficiency. Very power-hungry transport cycles may require more energy than the genset can supply in nonstop maximum efficiency operation. In that case, a decision must be made between most efficient operation (compromised performance) and high-performance operation (compromised efficiency) at the genset's maximum power point.

Figure 11 shows again all main subsystems of the hybrid drivetrain, their interconnections and the way different flows of energy among these subsystems are modeled. P_{Required} constitutes the total mechanical power of the mainline drive and haulback drive, both computed based on cable force and speed in the respective work phases, as described by Eq. 3. Losses within the reduction gearing should be quite small and have therefore been ignored. Losses of the electric drives (electric motor/generator and a dedicated inverter) are summarized as a total efficiency denoted by η_{EL}. This limited efficiency leads to the electric power at the PDU output being larger than the mechanical power at the drives if the drive is in motoring mode and for it being smaller in case of generator mode. This is indicated by the expressions next to the respective arrows of energy flow in Fig. 11. At the PDU, electric power of the mainline and haulback drives combines

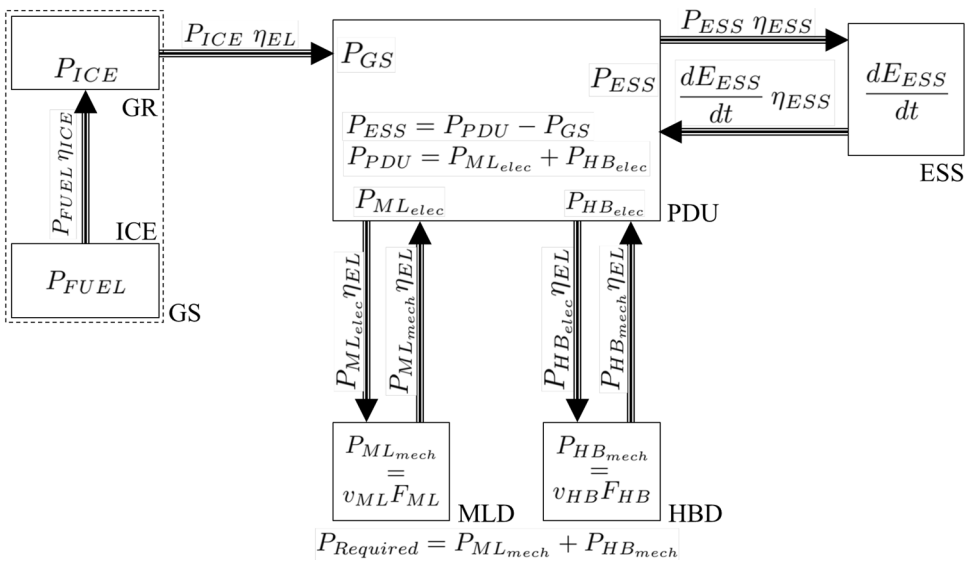

Fig. 11 Model of hybrid drivetrain main subsystems. The variables are defined as follows: P_{FUEL}—fuel flow rate equivalent power; η_{ICE}—combustion engine efficiency; P_{ICE}—combustion engine power (mechanical output power); η_{EL}—efficiency electric motor/generator and inverter (power electronics); P_{GS}—genset power; P_{ESS}—power energy storage system; η_{ESS}—energy storage system charge and discharge efficiency; $\frac{\mathrm{d}E_{\text{ESS}}}{\mathrm{d}t}$—rate of change of energy stored in the energy storage system; P_{PDU}—total electric power delivered via the power distribution unit; $P_{ML_{\text{elec}}}, P_{HB_{\text{elec}}}$—electric power of the mainline and haulback drive, respectively; $P_{ML_{\text{mech}}}, P_{HB_{\text{mech}}}$—mechanic power of the mainline and haulback drive, respectively; $v_{\text{ML}}, v_{\text{HB}}$—cable speed of the mainline and haulback winch, respectively; $F_{\text{ML}}, F_{\text{HB}}$—cable force of the mainline and haulback winch, respectively; P_{Required}—total mechanical power needed to power the yarding process

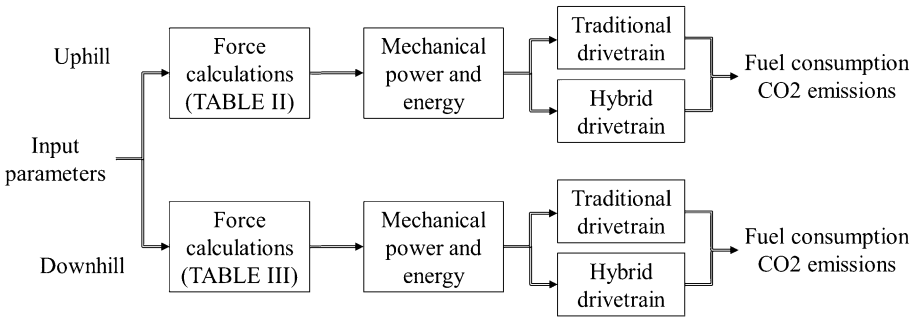

Fig. 12 Model simplified simulation scheme

Table 4 Model general input parameters

Parameters	Value	Parameters	Value
Carriage mass (kg)	700	Elevation difference (m)	100
Load mass (kg)	3000	Time loading (s)	90
Length corridor (m)	500	Time unloading (s)	60
Distance tower yarder—load (m)	300	Hook speed unloaded (m/s)	2
Loading height (m)	4	Payload lifting speed (m/s)	1
Unloading height (m)	4	Payload lowering speed (m/s)	1.5
Lateral yarding distance (m)	30	Counteracting force haulback line (N)	3000
Friction coefficient load-ground (–)	0.6	Counteracting force main line (N)	3000
Friction coefficient cable-ground (–)	0.4	Line deflection (β) (°)	20
Carriage speed loaded (m/s)	3	Log length (m)	4.2
Carriage speed unloaded (m/s)	8	Cable length carriage-hook	2
Mass per meter of cable (kg/m)	0.64		

to P_{PDU}. If active, the genset provides electric power P_{GS} to the system (at the PDU). Part of the engine power P_{ICE} is lost due to the limited efficiency of the generator–inverter set, also assumed to be η_{EL}. Limited engine efficiency η_{ICE} results in an even higher power flow based on the fuel consumption rate, denoted as P_{FUEL}. The energy storage system serves as an energy buffer, whose terminal power P_{ESS} can be computed as the difference of P_{PDU} (power of the load) and P_{GS} (source power). If P_{ESS} is positive, the energy storage system is discharged. The rate of energy discharge ($\frac{dE_{ESS}}{dt}$) from the energy storage system is larger than the power output at its terminals, modeled by considering coefficient η_{ESS}. In case the power is negative, the storage system is charged. Again, losses occur and the rate at which energy is stored in the system is smaller than could be expected by the terminal power.

Hypothesizing that the average chemical composition of diesel is $C_{12}H_{23}$, which varies depending on the country, supplier and period of the year, it was possible to estimate that for each liter of fuel burned approximately 2.624 kg of CO2 are produced. This allows to make a connection between fuel savings and CO2 reduction in the subsequent discussions. The calculation was done using the oxidation reaction and assuming complete combustion. This is a good approximation for this type of calculation in diesel engines, where the amount of air is considerably higher than in stochiometric combustion.

Table 5 Hydraulic and hybrid powertrain characteristics

Parameters	Hydraulic	Electric
Drive train efficiency (–)	0.6	0.85
Max. engine power (kW)	300	40
Engine speed at rated power (rpm)	2200	2800
Volumetric energy density of diesel (MJ/l)	38.6	38.6
Idling power (W)	3000	–
Nominal efficiency of the engine (–)	0.41	0.41
Engine rotational speed during operation (rpm)	1800	–

Model implementation

The tower yarder model was built in MATLAB, while the input parameters are given through an Excel file. The first step of the model is to identify if the simulation corresponds to an uphill or downhill configuration. Based on that, the forces related to the transport cycle, defined by the input parameters, are calculated. Following this, the corresponding mechanical power and energy need are computed. The model then estimates the energy and fuel requirements of

two different powertrain configurations: traditional and hybrid, together with their environmental impact. A simplified outline of the model's calculation procedure is presented in Fig. 12.

In Table 4 are reported the general characteristics given as an input to the tower yarder system of this work, while in Table 5 the parameters of both powertrain types: traditional and hybrid are presented. In Table 5, it can be noticed how for the hybrid powertrain no idling power is presented. This is due to the logic of this system that will turn off the engine when it is not in use. This avoids unnecessary consumption and emissions. In a similar way, no engine working speed is reported, since a characteristic of series hybrid powertrains is that the speed of the engine is decoupled from the load, so the engine can work at its maximum efficiency point, differently to what occurs in the traditional system, where the speed is fixed depending on the system, but the torque varies depending on the instantaneous power need. Another important aspect that should be noticed is how the engine of the traditional system is considerably bigger than the one of the hybrid systems, which makes its nominal speed to be lower. The engine in the hybrid tower yarder must cope with the average cycle power, while in the conventional setup it must be able to supply the peak power. In hybrid configuration, the energy storage system should be able to provide the remaining power to guarantee performance.

Simulation results and discussion

Simulations of a tower yarder running two typical logging cycles, one uphill and one downhill, with the characteristics of Table 4 were performed. In this section, the results of the simulations with the two powertrain configurations (5) are presented.

Uphill

The performance of the conventional tower yarder is presented in Fig. 13a. Each work phase's duration in uphill and downhill configuration is computed from cable speed and the distance to be covered by the winches within the respective work phases. Results are reported in Table 6. The required power refers to the mechanical power needed by the system to operate as desired (black trajectory). In the first work phase (from 0 to t1), the required power is negative because the carriage is moving downhill thanks to gravity force. This braking energy could in theory be recovered, if the powertrain allowed for it. Similarly in work phase 2 when the hook is lowered, the mechanical power continues to be negative. Power is very small and is caused by the weight of the cable. When attaching the load in work phase 3, the system does not require any power to work. In conventional powertrains, the engine is not turned off and operates at idling speed. A similar situation occurs in work phase 7. At the beginning of working phase 4, force peaks commonly occur to get the immobile load to start moving,

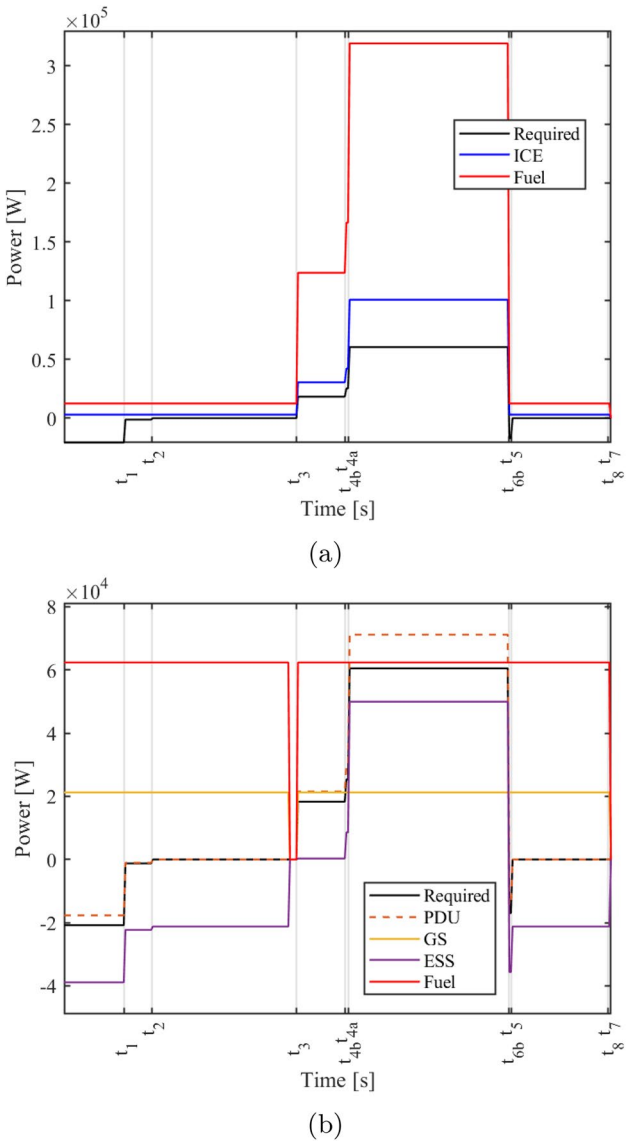

Fig. 13 Power curves of the hydraulic (**a**) and hybrid (**b**) systems in uphill configuration

Table 6 Cumulative duration of the transport cycle's work phases

$0-t_i$	t_1	t_2	t_3	t_{4a}	t_{4b}	t_5	t_{6a}	t_{6b}	t_7	t_8
[s]	37.5	54.5	144.5	174.5	176.5	276.5	276.5	277.8	337.8	339.8

to overcome the force of gravity and, especially, friction and possible hangups. During this breakout, phase cable speed is generally still small, such that the winch power is not large yet. Since this period is usually very brief, these complex dynamics have been ignored by the model. The mechanical power in work phase 5 from t4b to t5 is positive, and large power is drawn by the system. This was expected, since the carriage is fully loaded and it is pulled uphill against gravity forces. In work phase 6, some additional power could be recovered as the load is lowered. The blue trajectory represents the power that the engine should supply to the system after the hydraulic drive's efficiency has been factored in. The red curve is the power released in the fuel combustion, before factoring in engine efficiency. The low efficiencies that characterize conventional powertrains can be seen in the big gaps that separate the curves. Moreover, it can be observed how the engine power is always positive, because the system is not designed for regenerative power. When mechanical power is negative the engine remains at idling conditions.

Figure 13b shows the power curves of the hybrid system. The required power (black curve) is the same as in the previous case. The first point that should be noticed is how the PDU power curve follows the required power because of the capability of the hybrid powertrain to regenerate power. The energy storage system is charged in the first three work phases. In work phase 5 (from $t4_b$ to $t5$) when the load is carried uphill, the energy storage system helps the genset to provide the required power. In this case, it is actually providing most of the power. 50 kW is provided by the energy storage system compared to the approximately 21 kW by the genset. The genset (yellow curve) works at its maximum efficiency point at all times, and in this simulated condition it is required to run almost nonstop. This means its maximum efficiency power is just slightly higher than the average net power required by the system. Accordingly, the engine in the hydraulic tower yarder just works for the same time span as the genset in the hybrid tower yarder. Genset engine efficiency is significantly higher, making the fuel combustion power one order of magnitude lower as compared to the hydraulic case.

Table 7 shows a comparison between both powertrains. The average engine efficiency of the hydraulic tower yarder is almost 0.14 points lower than the engine efficiency of the electric tower yarder. This helps to explain why there is a 45% reduction in fuel consumption and greenhouse emissions. In the hydraulic case, the engine should be ON the complete cycle, whereas, in theory, it could be OFF for 4 s in the electric case. These results confirm what is observed in Fig. 13a: the current size of the engine in the conventional tower yarder makes it work far from its maximum efficiency region, thus increasing the environmental impact of the system.

Downhill

The mechanical power of the mainline and haulback lines is presented in Fig. 14a, together with the power that the hydraulic and electric system should manage. In the hydraulic case, there is no negative power, since in the conventional configuration this power is dissipated, and the system only provides the positive power required by the mainline or haulback line. On the other hand, in the hybrid configuration the system can recover part of the braking power and, therefore, the power to be provided is the sum of both line's power. Similar to the analysis that were done for the uphill case, in Fig. 14a it can be observed that in work phase 1 the haulback power is positive in order to pull the carriage up, while the mainline power is negative to tension the cables in order to guarantee their correct winding and unwinding. Since the hook does not lower itself anymore by gravity as in the previous case, the power in work phase 2 is positive. Specifically, the mainline provides the motion power, while the haulback line guarantees the correct winding of the cables. As before, when the load is getting attached and detached (work phase 3 and work phase 7), the power is 0. There is a "peak" of power when the load is being lifted (work phase 4-b) because the system should act against the gravity and pre-tension forces combined. In work phase 5, the signs of mainline and haulback power are inverted as compared to the work phase 1 case, since the loaded carriage is moving downward. Each work phase's duration is reported in Table 6.

In Fig. 14b, the power curves of the conventional powertrain are presented. Similar observations to the uphill case can be made. The engine efficiency is low also in this case, which is given by the big gap in between the engine (blue) and fuel combustion (red) power curves. In this case,

Table 7 Powertrain performance comparison—uphill and downhill transport

	Uphill			Downhill		
	HY	EL	Imprv (%)	HY	EL	Imprv (%)
Fuel consumption (l/cycle)	0.998	0.543	44.6	0.839	0.307	63.4
CO2 emissions (kg/cycle)	2.615	1.426	45.5	2.203	0.845	61.6
Av. engine efficiency (–)	0.264	0.400	51.5	0.251	0.400	59.4
Time engine ON (s)	340	336	1.2	340	190	44.1

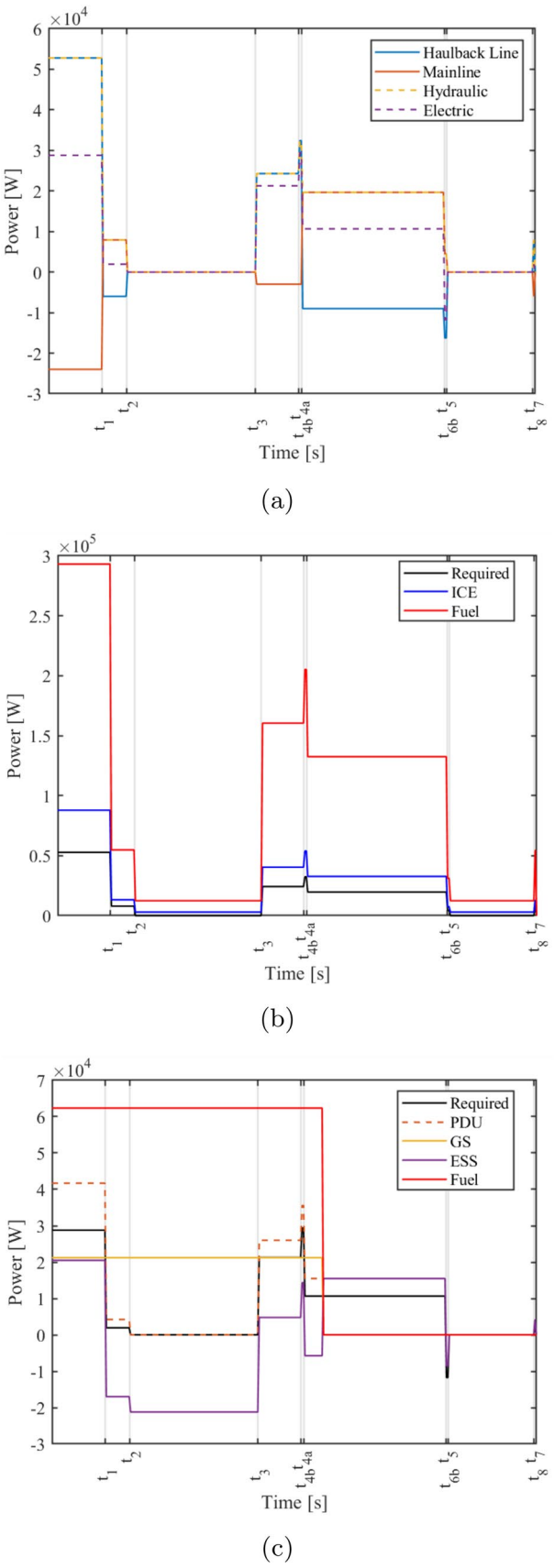

Fig. 14 Power curves of the mechanical (**a**), hydraulic (**b**) and electric (**c**) systems in downhill configuration

there is always a drum that requires power to make the system move. This explains why the engine power is always higher than the idling power, unless in the attaching and detaching phases. Figure 14c shows the performance of the electric powertrain in downhill configuration. In this case, both power sources help to bring the carriage uphill. In work phases 2 and 3, the battery is charged by the genset, which works for 190 s (Table 7) at its maximum efficiency point to provide the total amount of energy required to run a complete cycle. From a certain point in work phase 5, the energy storage system has stored enough energy to run the rest of the cycle on its own. The time the genset should be ON decreases with the possibility of energy recovery. Also in this case, the maximum power of the engine in hybrid configuration is one order of magnitude lower than in the conventional case. Table 7 shows that the potential reduction in fuel consumption and greenhouse emissions for this configuration is around 63%, much higher than in the uphill case. This was expected because at the beginning the logs have a higher potential energy compared to the final state, which constitutes energy to be recovered. More energy could be recovered if friction losses are reduced. In case of hydraulic tower yarders, loop-pretension is directly linked to energy loss. In the hybrid tower yarder, only part of the power associated with pre-tensioning is lost due to cable friction and limited system efficiency, while the remaining part can be recovered (see Table 3).

The average efficiency of the conventional tower yarder engine is again rather low (25%), confirming the fact that hybridization could be a suitable solution to downsize the engine and ensure higher efficiency. Even a reduced downsizing, not like the one presented in this work, could achieve considerable results in terms of fuel consumption and environmental impact.

Sensitivity analysis

The duty cycle parameters used in the previous section were defined based on experience as an average of the conditions for logging in South Tyrol, Italy. The aim of this section is to understand how variations in these conditions can affect the energy required by the system and the potential for powertrain electrification. The studied parameters are: load mass, load height, friction coefficient between load and ground as well as elevation difference. The sensitivity analysis was run separately for each configuration: uphill and downhill. For the latter, the effect of the pre-tensioning force and the friction between the ground and the cable was also studied.

The impact of additional variables as the loading distance and carriage speed could also be studied, but for the sake

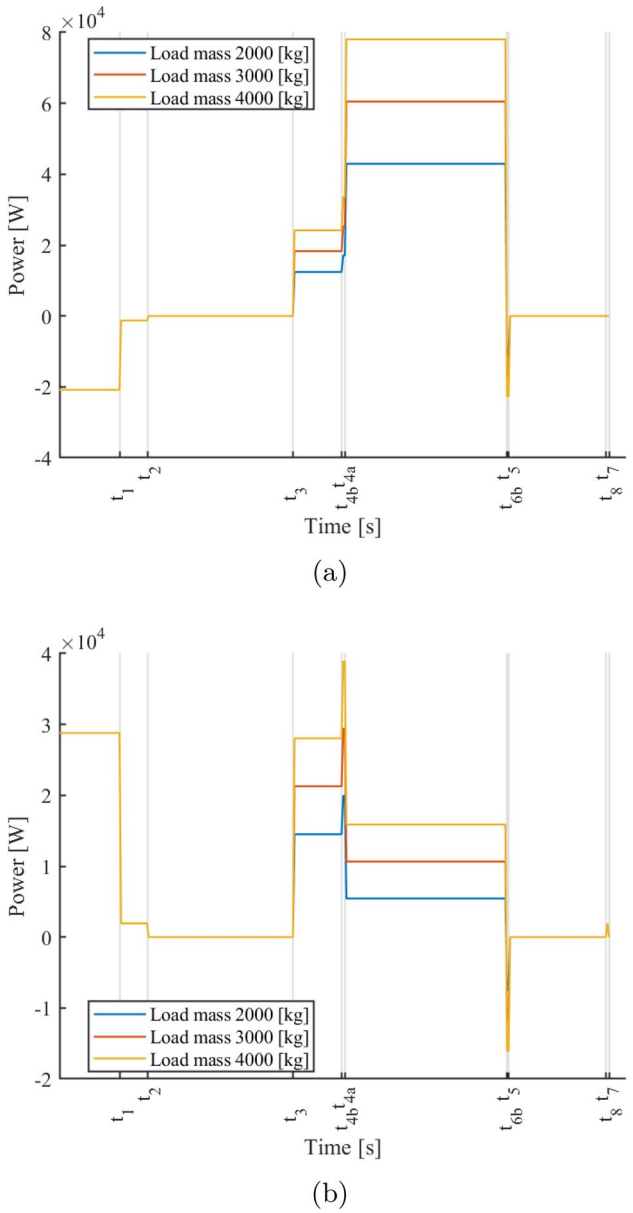

Fig. 15 Sensitivity analysis: load mass effect on total tower yarder power in uphill (**a**) and downhill (**b**) configuration

of conciseness they have been excluded from this work. In any case, it is expected that changing the loading distance will not change the maximum power required but only the total energy. The latter will probably require the ICE to run longer, in some cases even out of its maximum efficiency point. In any case, loading distance is expected to have a higher impact in terms of productivity (Lee et al. 2021). On the other hand, the velocity would probably alter the power, but the energy required would just slightly vary depending on the friction losses.

Load mass

The first parameter studied was the mass of the load, which does not affect any of the work phase's duration and, thus, neither the duration of the cycle, neither in uphill or downhill configuration. The results for uphill transport are presented first. Figure 15a reports a comparison of the power curves using the three values of mass. As expected, the power only changes after the load has been attached to the system (starting at work phase 4). Table 8 presents the fuel consumption and average efficiency for the conventional powertrain and the fuel consumption for the hybrid powertrain. The relationship between load mass and fuel consumption is not linear, which is due to the increase in engine efficiency when the load is closer to the rated engine power. This means that, for the conventional powertrain configuration, it is beneficial to load the system as much as possible, obviously according to the power limits of the tower yarder and cable load capabilities. On the other hand in the hybrid configuration, when the load increases, and thus the required power, the engine is no longer able to provide the cycle energy when working at the maximum efficiency point. Therefore, the engine worked at its maximum power point with a lower efficiency, making the consumption relatively higher and reducing the convenience of the hybrid configuration.

Similar results were obtained for downhill configuration (Fig. 15b). In this case, it seems that the pre-tensioning force governs the behavior of the system because the change of mass barely changes the efficiency of the engine, which depends on the load factor. For the hybrid powertrain, the change of fuel consumption is proportional to the duration

Table 8 Sensitivity analysis: load mass effects

	Load mass (kg)					
	2000	3000	4000	2000	3000	4000
	Uphill			Downhill		
Fuel consumption (l/cycle)	0.799	0.998	1.160	0.717	0.839	0.953
Av. engine efficiency (–)	0.253	0.264	0.275	0.249	0.251	0.253
Fuel consumption HY (l/cycle)	0.368	0.542	0.901	0.241	0.307	0.373
Fuel savings (%)	53.9	45.7	22.3	66.4	63.4	60.9

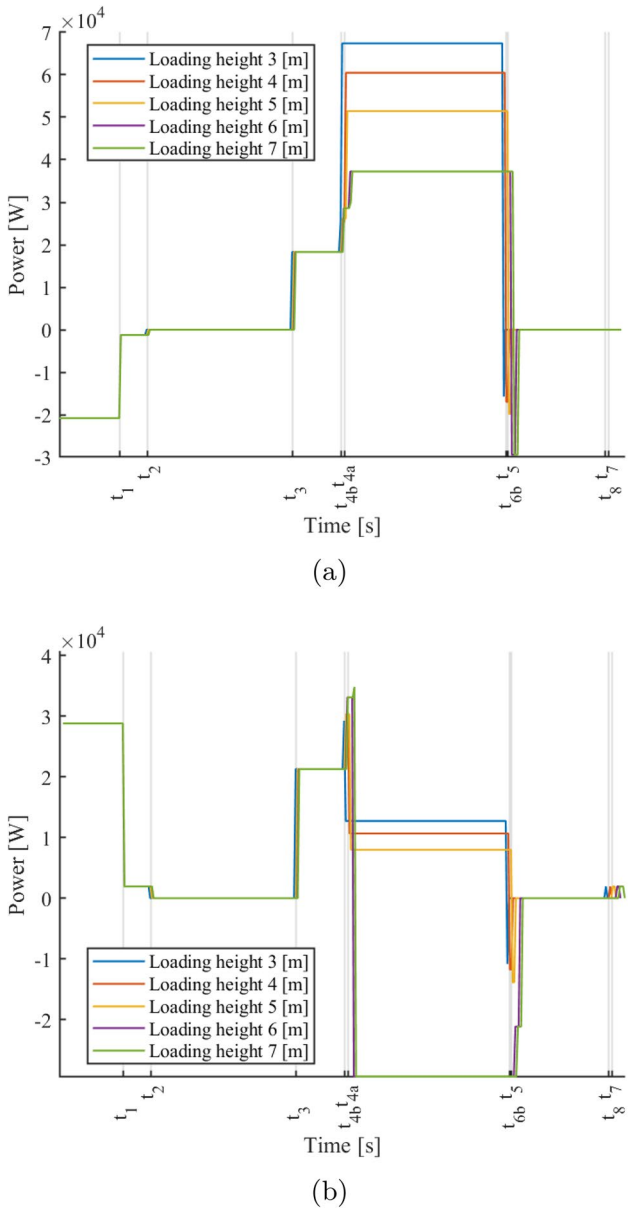

Fig. 16 Sensitivity analysis: loading and unloading height effect on total tower yarder power in uphill (**a**) and downhill (**b**) configuration

it must be on, since the engine works always at its maximum efficiency point.

In general, it seems that when the load increases and becomes closer to the nominal power of the conventional powertrain, the benefits of hybridization become smaller. This is because the efficiency of the combustion engine in a conventional yarder increases with increasing load factor, while the engine in the hybrid yarder runs load independent at the maximum efficiency point. Optimizing efficiency thus also comes down to proper equipment sizing with respect to the task at hand. In the lowest case simulated, the fuel consumption savings are estimated to be around 22%.

Table 9 Sensitivity analysis: loading and unloading height effects

	Loading and unloading height (m)				
	3	4	5	6	7
Uphill					
Fuel consumption (l/cycle)	1.048	0.998	0.924	0.777	0.783
Av. engine efficiency (–)	0.268	0.264	0.258	0.251	0.250
Fuel consumption HY (l/cycle)	0.758	0.5420	0.463	0.336	0.337
Fuel savings (%)	27.7	45.7	49.9	56.8	57.0
Downhill					
Fuel consumption (l/cycle)	0.865	0.839	0.803	0.674	0.682
Av. engine efficiency (–)	0.251	0.251	0.250	0.249	0.249
Fuel consumption HY (l/cycle)	0.323	0.307	0.286	0.026	0.028
Fuel savings (%)	62.6	63.4	64.4	96.1	95.9

Loading and unloading height

Figure 16a, b shows the power curve for different loading and unloading heights. The system consumes less energy when the load is fully lifted as for 6 m and 7 m. This indicates that the energy dissipated along the extraction path due to friction is higher than the energy to completely lift the load. This result could vary depending on the friction coefficient, but the value assumed in this work should represent a typical condition. In addition, the results in Table 9 suggest that there exists a minimum point of consumption. Below a certain height the friction increase due to the higher contact force when moving along the path is less than the energy increase for lifting the load further from the ground. On the other hand, lifting the load beyond complete suspension does of course not provide additional benefits. The minimum height for the current configuration is between 5 and 6 ms, but this should vary depending on the terrain, the slope, the transportation distance and the length of the logs. The importance of these results lies in the fact that this parameter can be regulated by the operator; in other words, it is an effective way to reduce consumption. Anyway, several other factors such as operator safety and risk of machine damage should be considered in the downhill case. Moreover, the reduction in the cycle average power (same trend than the fuel consumption) makes the hybrid system more attractive. In fact, if fully suspended, the system is almost autarkic, achieving a fuel saving of up to 96.1%.

Table 10 Sensitivity analysis: ground load friction coefficient effects

	Friction coefficient (–)			
	0.3	0.6	0.7	0.9
Uphill				
Fuel consumption (l/cycle)	0.869	0.998	1.033	1.093
Av. engine efficiency (–)	0.258	0.264	0.266	0.269
Fuel consumption HY (l/cycle)	0.434	0.542	0.720	0.788
Fuel savings (%)	50.1	45.7	30.3	27.9
Downhill				
Fuel consumption (l/cycle)	0.606	0.839	0.936	1.090
Av. engine efficiency (–)	0.248	0.251	0.253	0.257
Fuel consumption HY (l/cycle)	0.139	0.307	0.363	0.461
Fuel savings (%)	77.1	63.4	61.2	57.7

Table 11 Sensitivity analysis: elevation difference effect

	Elevation difference (m)				
	60	80	100	120	140
Uphill					
Fuel consumption (l/cycle)	0.911	0.957	0.998	1.035	1.069
Av. engine efficiency (–)	0.258	0.261	0.264	0.267	0.269
Fuel consumption HY (l/cycle)	0.476	0.510	0.542	0.721	0.757
Fuel savings (%)	47.7	46.7	45.7	30.3	29.2
Downhill					
Fuel consumption (l/cycle)	1.008	0.931	0.839	0.734	0.686
Av. engine efficiency (–)	0.254	0.252	0.251	0.250	0.251
Fuel consumption HY (l/cycle)	0.401	0.355	0.307	0.257	0.221
Fuel savings (%)	60.2	61.9	63.4	65.0	67.8

Ground load friction coefficient

Terrain morphology, composition and humidity can strongly affect the terrain friction coefficient. Different results can likely be obtained for whole-tree yarding versus harvesting cut-to-length logs with or without limbs. The general trends, however, are likely the same. Since it is difficult to identify a typical friction coefficient value from field experience, a wide range has been studied to include all possibilities. In general, the fuel consumed increases with the friction coefficient and it seems to play a more important role for the hybrid configuration, probably because in this case friction losses represent a relatively large part of the total energy required for the cycle. Friction losses in the conventional yarder may in some instances have no effect, as they may simply result in smaller mooring losses. In the hybrid tower yarder on the other hand, such energy could otherwise be recovered and therefore constitutes direct losses. In the hybrid system, fuel consumption can increase by 45% in uphill configuration, and by 50% in downhill configuration, when the friction coefficient increases from nominal 0.6 to 0.9 (constituting a 50% increase). Despite this strong dependence, hybridization is attractive independent of the friction term since consistent energy and environmental benefits were obtained in all the conditions (see Table 10). This suggests that hybrid yarders are an attractive solution to safe fuel in whole-tree and cut-to-length extraction.

Elevation difference

The difference in elevation can be related to the slope of the system, since the distance remains unchanged. The uphill and downhill configurations have opposite behavior with the change of the slope. An increase in the angle will favor and hinder the movement in the downhill and uphill configurations (work phase 5), respectively. Of the transport operation

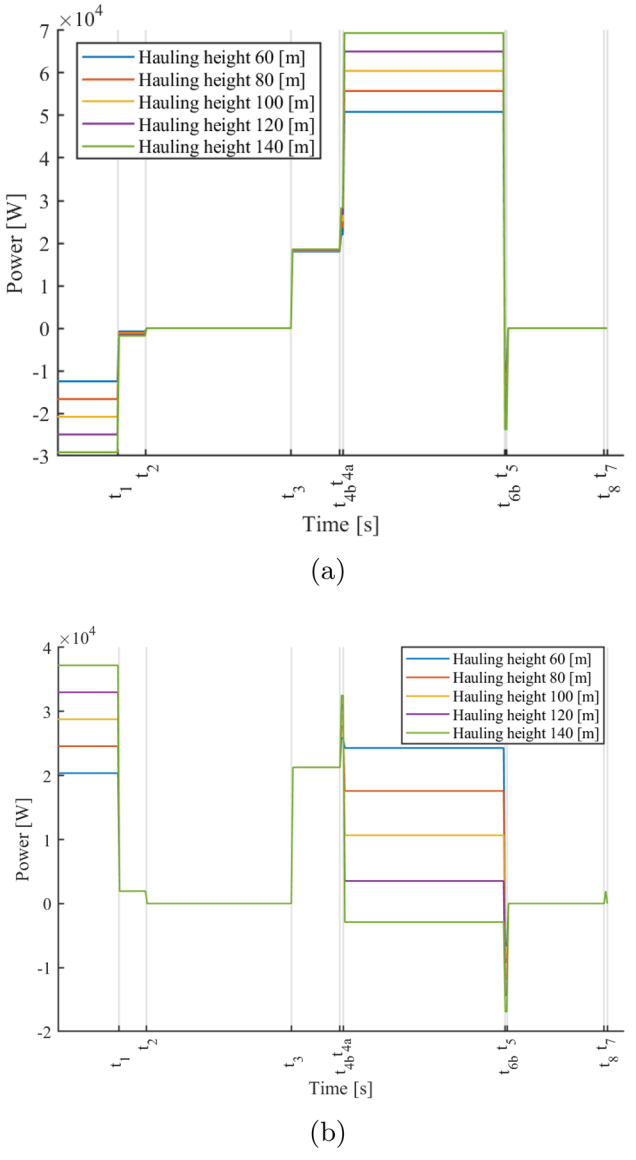

Fig. 17 Sensitivity analysis: elevation difference effect on total tower yarder power in uphill (**a**) and downhill (**b**) configuration

Table 12 Sensitivity analysis: ground cable friction coefficient effect

	Friction coefficient (–)		
	0.2	0.4	0.6
Downhill			
Fuel consumption (l/cycle)	0.772	0.839	0.912
Av. engine efficiency (–)	0.249	0.251	0.253
Fuel consumption HY (l/cycle)	0.262	0.307	0.357
Fuel savings (%)	66.1	63.4	60.9

Table 13 Sensitivity analysis: pre-tensioning force effect

	Pre-tensioning force (N)			
	2000	2500	3000	3500
Downhill—mainline force				
Fuel consumption (l/cycle)	0.791	0.816	0.839	0.861
Av. engine efficiency (–)	0.248	0.249	0.251	0.252
Fuel consumption HY (l/cycle)	0.289	0.298	0.307	0.316
Fuel savings (%)	63.5	63.5	63.4	63.3
Downhill—haulback force				
Fuel consumption (l/cycle)	0.766	0.803	0.839	0.875
Av. engine efficiency (–)	0.250	0.250	0.251	0.251
Fuel consumption HY (l/cycle)	0.289	0.298	0.307	0.316
Fuel savings (%)	62.3	62.9	63.4	63.9

cycle, work phase 5 is likely the most critical one in terms of fuel consumption. In the uphill case, the engine of the hybrid configuration works at its maximum power when the elevation is 120 m and 140 m, reducing the benefits of this type of powertrain. On the other hand, in the downhill case the fuel needed by both configurations decreases with the increase in the elevation difference. This is because in the conventional powertrain the weight helps the movement downhill, so less energy is required, while in the hybrid system it is also because of more energy that can be recovered because the braking force on the haulback line must increase to contrast gravity. The advantage of the hybrid setup over the conventional configuration therefore increases with skyline slope in downhill extraction. The convenience of the hybrid powertrain is evident in all the cases, since the minimum fuel consumption reduction estimated was about 29 %. Table 11 shows how these benefits are more variable in the uphill configuration.

The change of the slope produces variations in the lifting angle of the load, but these do not have any significant impact in terms of energy and thus fuel consumption, as can be seen in Fig. 17a, b.

The subsequent parameters just apply to the downhill configuration.

Ground cable friction coefficient

Similar to the results obtained for the friction coefficient between load and ground, the power required increases with the friction coefficient between ground and cable. Engine efficiency of the conventional powertrain slightly increases. Anyway, variations of 50% of the ground cable friction coefficient produce variations in 8% in the fuel consumption of the conventional powertrain and a maximum of 16% for the proposed hybrid drivetrain. This means that the impact of the parameter on the fuel consumption is quite small, at least with the given selection for the deflection angle. Detailed results are reported in Table 12.

Pre-tensioning force (haulback line and mainline—only in downhill yarding)

Table 13 reports the fuel consumption of the tower yarder when the conventional and hybrid powertrains are used and the pre-tensioning force is varied. Note that a change in pre-tensioning force may be required due to a change of skyline slope, showing the relation to the results in chapter Sect. 5.3.4. Results are reported for pre-tensioning forces in the range of 2–3.5 kN. In the upper half of the table, only the pre-tensioning force imposed by the mainline drive is varied, while the same of the haulback drive is kept at a constant value of 2.5 kN. Equivalent results are reported for variable haulback drive pre-tensioning force in the bottom half of the table. In the conventional powertrain, an increase in the pre-tensioning force can be directly translated to extra energy necessary for the cycle, as the energy associated with the retarding movement is dissipated via the mooring valves. When the hybrid configuration is used, most of this energy can be recovered, leading to smaller pre-tensioning sensitivity. Not reported are results of the combined variation in haulback drive and mainline drive pre-tensioning forces. It is, however, reasonable to expect that the results with individual variation can be superimposed with reasonable accuracy. Even though the impact on the hybrid configuration is limited, the optimization of this force can easily reduce the overall fuel consumption.

Conclusion

A conventional hydraulic tower yarder and a proposed hybrid tower yarder system were investigated via simulation. Models were developed of the cable-based transport process uphill and downhill. The models estimate the mechanical force and power requirements of the transport cycle, as well as the fuel consumption and greenhouse emissions for each powertrain configuration. Simulation results confirm that there is significant potential to reduce the fuel consumption

and emissions by means of hybridization. Simulations based on common transport characteristics revealed a 63 % saving when transporting downhill and 45% when transporting uphill, despite performing the same mechanical work on the harvested load. These savings are thus solely brought by via increased transport efficiency, made up by higher drivetrain efficiency, engine operation at the maximum efficiency point and energy recovery whenever a drive is in generator mode. Further extensive sensitivity analysis predicted that the proposed hybrid concept remains effective under largely varying transport conditions, such as varying payload mass, skyline height, ground friction of payload and cables, skyline slope and cable pre-tensioning in the downhill setup. Results showed that aspects like ground friction have a larger negative impact on the hybrid tower yarder, while cable pre-tensioning force increase for instance makes the hybrid concept even more attractive. The benefit of hybridization resulted in at least 22% fuel savings under the worst-case scenario simulated and is thus promising. Despite simulating a wide range of transport characteristics, these results cannot be deemed to be representative for all relevant conditions in practice. In addition, the effects of an array of simplifications made during the modeling stage also have in some degree an impact on these results. Further analysis and practical tests are needed to confirm these case study results by comparing simulated data with real-world measurements. Modern tower yarders are already equipped with suitable operational monitoring systems that can objectively measure the work patterns carried out (phases and intensity of the transport cycles performed). Hybrid drivetrains per default incorporate an array of sensors to accurately track torque, speed, power, energy consumption, temperature etc. of the drives, as well as the state of charge, state of health, energy throughput, etc. of the energy storage system. This makes it possible to optimize these solutions to the growing requirements of traceability in the sector, satisfying possible process certification functions that are becoming more and more pressing among the technological Precision Forestry applications.

Author contributions SL, MP, MR and RV designed the research layout. SL and MP modeled the system, performed simulations and wrote the manuscript. MR and RV provided guidance, discussed the results and contributed to the manuscript. All authors edited and revised the final manuscript.

Funding Open access funding provided by Libera Università di Bolzano within the CRUI-CARE Agreement. This work has been partially supported by the project "FiRST Lab: Field Robotics South-Tyrol Lab" (project number: FESR1084) funded under the European Regional Development Fund (ERDF) 2014-2020—Province of Bozen (I)-framework. The funding source had no involvement in study design; in the collection, analysis and interpretation of data; in the writing of the report; and in the decision to submit the article to the European Journal of Forest Research

Declaration

Conflict of interest The authors declare they have no conflict of interest.

References

Agwu Nnanna AG, Rolfs E, Taylor J, Ferreira KAF (2015) Experimental investigation of hydraulic-pneumatic regenerative braking system. In: ASME international mechanical engineering congress and exposition, proceedings (IMECE), vol 6A-2015

Ben-Chaim M, Shmerling E, Kuperman A (2013) Analytic modeling of vehicle fuel consumption. Energies 6(1):117–127

Cadei A, Mologni O, Marchi L, Sforza F, Röser D, Cavalli R, Grigolato S (2021) Energy efficiency of a hybrid cable yarding system: a case study in the north-eastern Italian alps under real working conditions. J Agric Eng 52(3):1185

Dalboni M, Santarelli P, Patroncini P, Soldati A, Concari C, Lusignani D (2019) Electrification of a compact agricultural tractor: a successful case study. In: ITEC 2019—2019 IEEE transportation electrification conference and expo

DEUTZ AG (2021) TCD 2011, For mobile machinery 23–74 .9 kW 31–100 hp at 1600–2800 rpm EU Stage IIIA/US EPA Tier 3

DieselNet (2021) EU: nonroad engines

EPA (2022) Regulations for emissions from heavy equipment with compression-ignition (diesel) engines

Gallo R, Visser R, Mazzetto F (2021) Developing an automated monitoring system for cable yarding systems. Croat J For Eng 42(2):213–225

Govardhan OM (2017) Fundamentals and classification of hybrid electric vehicles. Int J Eng Tech 3(5):194–198

Karlušić J, Cipek M, Pavković D, Benić J, Šitum Ž, Pandur Z, Šušnjar M (2020) Simulation models of skidder conventional and hybrid drive. Forests 11(9):921

Knobloch C, Bont LG (2021) A new method to compute mechanical properties of a standing skyline for cable yarding. PLoS ONE 16(8 August):e0256374

Kühmaier M, Harrill H, Ghaffariyan MR, Hofer M, Stampfer K, Brown M, Visser R (2019) Using conjoint analyses to improve cable yarder design characteristics: an Austrian yarder case study to advance cost-effective extraction. Forests 10(2):165

Lagnelöv O, Dhillon S, Larsson G, Nilsson D, Larsolle A, Hansson P-A (2021) Cost analysis of autonomous battery electric field tractors in agriculture. Biosyst Eng 204:358–376

Lee E, Choi Y, Cho M, Cho K, Oh J, Han S, Im S (2021) A literature review on cable extraction practices of South Korea: 1990–2020. Forests 12(7):908

Leitner S, Perez Estevez M, Renzi M, Vidoni R (2022a). Tower yarder energy efficiency study in logging operations: hydraulic

vs. hybridized drivetrain. In: 10th international conference on sustainable energy engineering and application, ICSEEA 2022; research organization for energy and manufacture; November 22–23, 2022, Puspiptek, Serpong, Tangerang Selatan, Indonesia
Leitner S, Renzi M, Spinelli R, Vidoni R (2022b) On the design of hybrid tower yarder drivetrains: a case study. Forests 13(9):1520
Matthews D (2021) Forestry 4.0 for improving yarder design and operations: a valentini yarder case study. M.Sc. Thesis, University of Canterbury, Christchurch, New Zealand, p 29
Medževepryte UK, Makaras R (2018) Drawbar performance of a hybrid agricultural vehicle. In: Transport means—proceedings of the international conference, vol 2018-October, pp. 1246–1249
Mendes FEG, Brandao DI, Maia T, Braz De Filho JC (2019) Off-road vehicle hybridization methodology applied to a tractor backhoe loader. In: ITEC 2019—2019 IEEE transportation electrification conference and expo
Mergl V, Pandur Z, Klepárník J, Kopseak H, Bačić M, Šušnjar M (2021) Technical solutions of forest machine hybridization. Energies 14(10):2793
Minderytė A, Pauraite J, Dudoitis V, Plauškaitė K, Kilikevičius A, Matijošius J, Rimkus A, Kilikevičienė K, Vainorius D, Byčenkienė S (2022) Carbonaceous aerosol source apportionment and assessment of transport-related pollution. Atmos Environ 279:119043
Mologni O, Lyons CK, Zambon G, Proto AR, Zimbalatti G, Cavalli R, Grigolato S (2019) Skyline tensile force monitoring of mobile tower yarders operating in the Italian Alps. Eur J For Res 138(5):847–862
Munteanu C, Yoshida M, Iordache E, Borz SA, Ignea G (2019) Performance and cost of downhill cable yarding operations in a group shelterwood system. J For Res 24(3):125–130
Pandur Z, Šušnjar M, Bačić M (2021) Battery technology—use in forestry. Croat J For Eng 42(1):135–148
Prochazka P, Pazdera I, Cipin R (2019) Hybrid tree harvester machine with battery powered hydro-electric drive. ECS Trans 95:349–354
Rong-Feng S, Xiaozhen Z, Chengjun Z (2017) Study on drive system of hybrid tree harvester. Scientific World Journal, Singapore
Schweier J, Klein M-L, Kirsten H, Jaeger D, Brieger F, Sauter UH (2020) Productivity and cost analysis of tower yarder systems using the Koller 507 and the Valentini 400 in southwest Germany. Int J For Eng 31(3):172–183
Shao Z (2021) The updated China IV non-road emission standards
Spinelli R, Marchi E, Visser R, Harrill H, Gallo R, Cambi M, Neri F, Lombardini C, Magagnotti N (2017a) The effect of carriage type on yarding productivity and cost. Int J For Eng 28(1):34–41
Spinelli R, Marchi E, Visser R, Harrill H, Gallo R, Cambi M, Neri F, Lombardini C, Magagnotti N (2017b) Skyline tension, shock loading, payload and performance for a European cable yarder using two different carriage types. Eur J For Res 136(1):161–170
Spinelli R, Visser R, Magagnotti N, Lombardini C, Ottaviani G (2020) The effect of partial automation on the productivity and cost of a mobile tower yarder. Ann For Res 63(2):3–14
Starkey MM, Williams RL II (2011) Capstan as a mechanical amplifier. In: Proceedings of the ASME design engineering technical conference, vol 6, pp 1309–1316
Talbot B, Stampfer K, Visser R (2015) Machine function integration and its effect on the performance of a timber yarding and processing operation. Biosyst Eng 135:10–20
Troncon D, Alberti L, Bolognani S, Bettella F, Gatto A (2019a) Electrification of agricultural machinery: a feasibility evaluation. In: 2019 14th international conference on ecological vehicles and renewable energies, EVER 2019
Troncon D, Alberti L, Mattetti M (2019b) A feasibility study for agriculture tractors electrification: Duty cycles simulation and consumption comparison. In: ITEC 2019—2019 IEEE transportation electrification conference and expo
Varch T, Erber G, Spinelli R, Magagnotti N, Stampfer K (2020) Productivity, fuel consumption and cost in whole tree cable yarding: conventional diesel carriage versus electrical energy-recuperating carriage. Int J For Eng 32:1–11
Zimbalatti G, Proto AR (2009) Cable logging opportunities for firewood in Calabrian forests. Biosyst Eng 102(1):63–68